

Executive Summary

On August 30, 1999, the South Florida Water Management District (District) contracted with DB Environmental Laboratories, Inc. (DBEL) to perform a 100-week evaluation of Submerged Aquatic Vegetation/Limerock (SAV/LR) Treatment System technology for reducing phosphorus (P) discharge from Everglades Agricultural Area (EAA) waters. The objectives of this project are to assess the long-term, sustainable performance of this technology, and to develop design and operational criteria for a full-scale SAV/LR system. For this effort, we are performing scientific and engineering work at Stormwater Treatment Area (STA)-1W at several spatial scales: outdoor microcosms and mesocosms, test cells (0.2 ha), Cell 4 (146 ha) and Cell 5 (1,100 ha). This document is a quarterly progress report describing work efforts of DBEL's project team from August - October 2000. Key accomplishments and findings are as follows.

During this quarter, we continued using existing mesocosms and test cells at both the North and South Advanced Treatment Technology (NATT and SATT) sites of STA-1W to assess effects of hydraulic loading rates, water type (Post-BMP vs. Post-STA), and system configuration on SAV/LR phosphorus removal performance. We also completed experiments on the stability of Cell 4 sediments during this quarter, and performed water column sampling in Cell 4 to characterize internal P concentration gradients. This spatial assessment was designed to assess impacts of both 'corrected' (plugged) and recently-formed short-circuits.

We initiated a long-term, flow-through microcosm study to assess the effects of soluble reactive P, calcium and alkalinity on P removal performance. SAV performance is being tested at high and low Ca (100 vs. ~20 – 30 mg/L) and alkalinity (375 vs. ~75 – 150 mg CaCO₃ /L) concentrations, as well as high (120 – 140 µg/L) and low (<20 µg/L) SRP concentrations. Eight microcosms containing *Najas guadalupensis* are receiving the various Ca/alkalinity and SRP media at a hydraulic loading rate of 9.6 cm/day (3.5 day hydraulic retention time).

During May, we initiated the fluctuating water depth study in NATT site mesocosms. In this experiment, water column depths for SAV mesocosms that previously had operated at steady state depths ranging from 0.4 to 1.2 m are being varied in a cyclical fashion. For this study, under "modified" depth regimes the water levels in the 0.4 m shallow mesocosms were raised

to 0.8 m, and the water in the 1.2 m deep mesocosms was reduced to 0.8 m. These “modified” depths were maintained for 5 weeks, after which time the water columns were returned to their original steady-state depths. After five depth fluctuation “cycles”, we subjected the mesocosms to one 5-week cycle at even shallower depths (0.15 and 0.4 m for the shallow and deep mesocosms, respectively) before returning the water depths to their “control” depths (0.4 and 1.2 m) for a final 3 week period. The typical fluctuations that were followed for five cycles did not appear to markedly affect P removal performance of the SAV communities. However, the final fluctuation cycle, where the water column was reduced to shallower depths, did result in increased outflow TP concentrations.

We continued operation of a pulse loading study, using SAV mesocosms that previously had received hydraulic loading rates (HLRs) of 11, 22 and 53 cm/day. Our hydraulic loading schedule for the mesocosms is similar to the “STA-2” hydraulic loading data set in the following respects: our protocol has the same average seasonal flow patterns; the same percentage of “no-flow” weeks; and, the same standard deviation on a seasonal basis. We have scaled (increased) the STA-2 HLRs by factors of 5X, 10X and 25X, with flow provided to the mesocosms in two-week long pulses. These increased flows were selected to match the prior, high HLRs (11 – 53 cm/day) to the SAV mesocosms, which should provide continuity with previous HLR studies.

To date, mesocosms subjected to moderate and low pulse-loading regimes are providing about the same outflow TP concentrations as those that receive a steady state loading. However, the highly loaded pulsed systems at times are subject to periods of poor performance. Under stagnant, “no-flow” conditions, we have periodically observed phytoplankton blooms in the mesocosms that receive Post-BMP waters at the higher HLRs (i.e., 22 and 53 cm/day).

To compare relative performance of SAV and cattail-dominated wetlands, we continued monitoring of shallow mesocosms containing these respective vegetative communities. The SAV mesocosms continued to outperform cattail mesocosms operated at similar depths (0.4m) and HLRs (10 cm/day), providing mean outflow TP concentrations of 39 and 65 µg/L, respectively, during the quarter.

We continued long-term monitoring of shallow (0.09 m deep) SAV/periphyton/LR raceways that receive Post-STA waters, as well as the deeper (0.4 m) tanks containing SAV cultured on muck, sand and limerock substrates. The shallow raceways followed by the “back-end” limerock beds continued to produce TP outflow concentrations lower than 10 µg/L for much of the quarter. In the substrate study, lowest outflow P concentrations were obtained in mesocosms with SAV cultured on a limerock substrate (12 µg/L), and highest outflow levels were observed with SAV cultured on a sand substrate (21 µg/L).

To test the effectiveness of various filter media as a “back-end” particle filtration step for SAV wetlands, we initiated a small-scale filtration study at the SATT site. We fabricated sixteen PVC columns that are being fed outflow water from SAV mesocosms. We are testing filter media that are inert, and therefore should only provide particulate filtration, as well as those with chemical characteristics (high calcium or iron content) that should further contribute to soluble P removal. Filter media being evaluated include: coarse (3.4 – 6.9 mm), medium (2.0 – 3.4mm) and fine (0.25 – 0.85 mm) quartz pebbles/sand; coarse and medium sized limerock; coarse and medium sized Ca/Mg silicate materials (Pro-Sil Plus™) ; and a fine, iron-coated quartz sand.

After eleven weeks (August 18 – October 30, 2000) of performance monitoring, we have observed slight decreases (3 – 5 µg/L) in the influent TP concentrations (mean of 18 µg/L) for the best performing media. Coarse and medium sizes of limerock and Pro-Sil Plus™ have proven to be the most effective filter media, removing primarily particulate P from solution. Calcium and alkalinity levels have been unaffected during passage through the filter media columns, except for the Pro-Sil Plus™ media, where both parameters have slightly decreased.

On August 9, 2000, we performed our second intensive water quality sampling within Cell 4. This provided an opportunity to evaluate the effectiveness of the structural modifications (i.e., limerock “plugs”) deployed by the District along the eastern and western levees to reduce hydraulic short-circuiting. Total and soluble reactive P concentration gradients for the 44-station grid revealed the presence of new short-circuits and the persistence of “dead” zones in the central part of the wetland. Additional sampling events in Cell 4 will be conducted during 2001.

Experiments to define the stability of Cell 4 sediments also were continued this quarter. We collected outflow sediments from this wetland, and subjected them to varying SRP, calcium, pH and redox conditions in our laboratory. We also performed sediment fractionations to determine the relative percentages of labile and recalcitrant sediment P pools, and to assess how the size of these pools change during the laboratory incubations. Having completed all the perturbation experiments for both inflow and outflow sediments, we found that lower labile P pools in the outflow sediment resulted in negligible release of SRP under oxic, low or high pH conditions, compared to SRP effluxes from the inflow sediments. However, SRP releases from the outflow sediment were comparable to those from the inflow sediment when both were dried and then reflooded. Contrary to the inflow sediment, anoxic conditions produced only a slight SRP release from the outflow sediment. Amending the overlying water with SRP to a concentration of 120 µg/L resulted in an immediate and almost complete removal of P by the outflow sediment, but only slight net removal by the inflow sediment. Finally, increasing the concentrations of calcium and alkalinity in the overlying waters had no effect on the SRP concentrations in the outflow sediment incubations, but there was an inhibitory effect on SRP release by the inflow sediment.

The 0.2 ha test cells are well into a post-recovery phase since the May 2000 limerock berm installation (south test cell [STC]-9 and north test cell [NTC]-15), and the SAV restocking and management in the other cells performed June - July 2000. Even though the cell flows were doubled to 11 cm/day in mid-September, both north test cells continued to improve with respect to P removal, providing outflow TP concentrations as low as 12 – 14 µg/L at the end of this quarterly reporting period. The presence of a limerock berm did not improve the P removal efficiency in the north test cells, but may have affected performance in the south test cells as STC-9 (containing the limerock berm) outperformed STC-4, with average outflow TP concentrations of 17 and 20 µg/L, respectively. Outflow TP concentrations from STC-9 declined to 11 µg/L during the last two weeks of this quarter.

The Dynamic Model for Stormwater Treatment Areas (DMSTA), an STA design model developed by consultants for the Department of Interior (DOI), was modified by us and then evaluated by comparing simulations from our version with the DOI version. Using the same input time series

and model parameters, the comparisons produced identical output. Using the DBEL model, we found that we could increase the goodness-of-fit measure by 50 – 100% if seasonal effects on TP removal (rather than velocity effects) are incorporated in a five-parameter model.

In August, we evaluated SAV colonization at the 120 monitoring stations that we had established in STA-1W Cell 5 during February 2000. Submerged vegetation, in particular *Najas* and *Ceratophyllum*, are continuing to expand throughout the wetland. Concomitant to this SAV spread, water column TP levels in Cell 5 outflow are declining (now < 50 µg P/L).

Table of Contents

Introduction	1
Task 5. Mesocosm Investigations	2
Effects of Calcium/Alkalinity and SRP Concentrations on P-Coprecipitation within SAV Beds.....	2
Variable Depth Mesocosms	5
Mesocosms for Long-Term Monitoring.....	6
The Effects of Pulse Loading and Drydown/Reflooding on P Removal Performance	10
Pulsed Loading.....	10
Sequential SAV/LR and Cattail Mesocosms	14
Sequential SAV/LR Mesocosms.....	14
Phosphorus Removal Efficiencies within Cattail- and SAV-Dominated Mesocosms.....	14
Shallow, Low Velocity SAV/Periphyton/Limerock Systems.....	16
Growth of SAV in Post-STA Waters on Muck, Limerock, and Sand Substrates	16
The Effects of Filter Media Type and Size on P Removal Performance	19
References	21
Task 6. Test Cell Investigations	22
Initial Performance of Test Cell Limerock Berms.....	22
Sediment Accretion Rates	24
Task 9. STA-1W Cell 4 Performance Monitoring and Characterization	26
Intensive Water Quality Sampling	26
Sediment P Stability/Release Experiments.....	29
Sediment Collection Methodology	29
Methodology for Sediment Stability Incubations.....	29
Desiccation Followed by Reflooding.....	30
High Ca and Alkalinity Concentrations	32
Soluble Reactive Phosphorus Amendments	34
Sediment P Fractions and Effects of pH and Oxidic vs. Anoxic Conditions on SRP Release from Cell 4 Outflow Sediment.....	36

Technical Evaluation of DMSTA for Simulating TP Removal in SAV Wetlands	38
Background.....	38
DMSTA Overview	39
Evaluation Methods.....	40
DMSTA water budget calibration	44
Calibration of DMSTA to Cell 4 TP data	44
Conclusions and Recommendations	49
References	50
Task 10. Cell 5 Inoculation and Monitoring.....	52

List of Figures

Figure 1.	Flow chart detailing the experimental design for the flow-through Coprecipitation Experiment.....	4
Figure 2.	Total P outflow concentration for static and variable depth shallow mesocosms (A) and static and variable depth deep mesocosms (B).....	7
Figure 3.	Total P outflow concentrations for static and variable depth mesocosms during final two months of study.	8
Figure 4.	Inflow and outflow total P concentrations for mesocosms receiving Post-BMP waters at HLRs of 11, 22 and 53 cm/day (7.0-, 3.5- and 1.5-day HRTs).....	9
Figure 5.	Outflow total P concentrations (mean, \pm 1 s.d) from mesocosms receiving Post-BMP waters at HLRs at 11, 22 and 53 cm/day (7.0- 3.5-, and 1.5-day HRTs).....	9
Figure 6.	Mean outflow total P concentrations from mesocosms that received high, moderate and low pulse loading regimes.....	12
Figure 7.	Outflow total P concentrations from mesocosms that received high, moderate and low flows of Post-BMP waters under pulsed and constant-flow regimes.	13
Figure 8.	Total P concentrations in the outflows of shallow (0.4 – 0.5 m depth) mesocosms dominated by cattail and SAV communities.....	15
Figure 9.	Total P concentrations in the influent and outflows of triplicate shallow, low velocity, SAV/periphyton raceways, and in the outflow of the subsequent limerock beds..	17
Figure 10.	Total Phosphorus concentrations in the influent and outflows of SAV mesocosms established on limerock, muck and sand substrates.	18
Figure 11.	Schematic of the column outflow structure used in the Filter Media experiment.....	20
Figure 12.	SRP release from the iron-coated sand filter column during Aug. 18-Oct 6, 2000.....	21
Figure 13.	Location of additional sampling stations (X) upstream and downstream of the LR berms in NTC-15 and STC-9.	22
Figure 14.	Total phosphorus concentrations in the influent and outflows of the North test cells during the August – October 2000 quarter.	24
Figure 15.	Total phosphorus concentrations in the influent and outflows of the South test cells during the August – October 2000 quarter.	25
Figure 16.	Internal transects in Cell 4 along which water quality (TP, SRP, pH, temperature) was evaluated at 44 stations on August 12, 2000.	27
Figure 17.	Total and soluble reactive phosphorus concentration gradients constructed from 44 stations internal to Cell 4 on August 9, 2000.	28
Figure 18.	Spatial gradients in total P concentrations within Cell 4 before (sampled December 17, 1999) and after (sampled August 9, 2000) the addition of limerock “plugs”.	28

Figure 19. The release of soluble reactive P (SRP) from the desiccation of Cell 4 inflow (a) and outflow (b) sediments over 99 and 72 hours, respectively, upon reflooding with Cell 4 outflow water.....	31
Figure 20. The release of soluble reactive P (SRP) from Cell 4 inflow (a) and outflow (b) sediments with Ca- and alkalinity-amended (75 – 76 mg Ca/L and 248 – 260 mg CaCO ₃ /L) Cell 4 outflow water.....	33
Figure 21. Soluble reactive P (SRP) concentrations for the SRP-amended and unamended overlying Cell 4 outflow water in contact with Cell 4 inflow (a) and outflow (b) sediments.....	35
Figure 22. Inorganic P fractionation of composited Cell 4 inflow and outflow region marl sediments.....	36
Figure 23. Time course for SRP release from Cell 4 outflow region marl sediments exposed to varying pH values.....	37
Figure 24. Time course for SRP release from Cell 4 outflow region marl sediments exposed to oxic and anoxic conditions.....	38
Figure 25. General model structure for DMSTA (Walker and Kadlec 2000a).....	40
Figure 26. Comparison of simulated G-256 outflow to daily measured data.	45
Figure 27. Comparison of simulated Cell 4 water depth to daily measured data.	45
Figure 28. DMSTA TP simulation using the first-order volumetric removal option for period of January 1995 through June 2000.....	46
Figure 29. DMSTA TP simulation using the first-order volumetric removal option for period of June 1997 through June 2000.....	46
Figure 30. Seasonal effect on TP removal.	48
Figure 31. Total phosphorus and apparent color concentrations of surface water near the outflow of Cell 5.	52

List of Tables

Table 1.	Final concentration of nutrients and micronutrients amended to W. Palm Beach tap water.....	4
Table 2.	Forty-week (Feb. 20 - Nov. 27, 2000) pulse loading schedule for low, medium, and high loaded mesocosms in Subtask 5v.....	10
Table 3.	Mean total phosphorus concentrations ($\mu\text{g/L}$) in the influent and outflows of pulsed and constant flow mesocosms receiving low, moderate and high loadings from February 21 – November 3, 2000.....	11
Table 4.	Comparisons between one SAV- and two cattail-dominated mesocosms at the NATTS in the removal of SRP, TSP, TP and alkalinity during the August – October 2000 period of record.	16
Table 5.	Mean total phosphorus concentrations (± 1 standard deviation) in the influent and outflows of duplicate substrate mesocosms during August - October 2000.	18
Table 6.	Filter media types and particle sizes used in the Filter Media Experiment (Subtask 5x).....	19
Table 7.	Mean (± 1 s.d.) TP, SRP, calcium and alkalinity concentrations in the influent and outflows of the Filter Media experiment (Subtask 5x) during the August 18- October 30, 2000 period of record.	20
Table 8.	Total, soluble reactive, dissolved organic, and particulate phosphorus concentrations ($\mu\text{g/L}$) at locations along the flow path in NTC-15 and STC-9 during the August – October 2000 quarter.....	23
Table 9.	Duration of desiccation, and before (initial) and after (final) dry:wet weight ratios and moisture loss, for the inflow and outflow sediments of Cell 4.	30
Table 10.	Dissolved calcium and alkalinity concentrations and specific conductance values in Cell 4 inflow and outflow waters before and after Ca/alkalinity amendments.	32
Table 11.	Summary of five sets of equations evaluated for DMSTA fluxes	41
Table 12.	Summary of variables and parameters for DMSTA.....	42
Table 13.	Summary of model calibrations for five options for DMSTA equations for period of 1/95 – 6/00..	47
Table 14.	Summary of model calibrations for five options for DMSTA for period of 6/97 – 6/00	47

Introduction

On August 30, 1999, the District contracted with DB Environmental Laboratories, Inc. (DBEL) to design, construct, operate, and evaluate a 100-week, multi-scale demonstration of SAV/Lime-rock Treatment System technology for reducing phosphorus (P) discharge from Everglades Agricultural Area (EAA) waters. The objectives of this project are to:

- Design and execute a scientific and engineering research plan for further evaluation of the technical, economic and environmental feasibility of using SAV/LR system for P removal at both the basin and sub-basin scale.
- Obtain samples adequate to conduct a Supplemental Technology Standard of Comparison (STSOC) analysis.
- Provide information and experience needed to design a full-scale SAV/LR system.

This document is a progress report for the fourth quarter describing work efforts during August – October 2000. This report focuses on methodology and findings from the mesocosm experiments (Task 5), test cell studies (Task 6), Cell 4 sediment stability, hydraulic analysis and performance model (Task 9) and Cell 5 inoculation studies (Task 10).

Task 5. Mesocosm Investigations

During the August – October 2000 quarter, we continued routine sampling of the following experiments at the North and South Advanced Treatment Technology sites: Variable Depth (Subtask 5ii), Long-Term Monitoring (5iv), Pulse Loading (5v), Sequential SAV/LR Systems and P Removal Efficiencies within Cattail- and SAV-Dominated Mesocosms (5vi), Long-Term P Removal by SAV/Periphyton Raceways (5vii), Substrate Effects on P Removal Performance (5ix), and Filter Media (5x). In addition to reporting the results of these on-going mesocosm experiments, we also provide descriptions of the experimental methodologies for two new investigations: Flow-Through Coprecipitation (5i) and Particle Characterization (5xi) studies.

Effects of Calcium/Alkalinity and SRP Concentrations on P-Coprecipitation within SAV Beds (Subtask 5i)

Findings from our Phase I research using Post-BMP waters suggest that P removal in an SAV system is controlled in part by water column hardness and alkalinity. Our initial batch experiment, which was reported in the Third Quarterly Report, entailed subjecting “P-enriched” and “P-deficient” *Najas* to a constant SRP concentration at high and low levels of calcium and alkalinity over a two-day measurement period. The aim of the experiment was to evaluate the relative importance of P uptake by SAV vs. coprecipitation of P in the water column. This experiment provided the first direct evidence that the P coprecipitation mechanism does occur within SAV beds. However, the rate and extent are predicated on the nutritional status of the SAV community and on the hardness of the water. Indeed, the removal of SRP within an SAV bed may depend more on the physiological needs and the nutritional condition of the vegetation than on the extent and amount of calcium carbonate precipitation.

Factors not explored in the short-term experiment, such as the effects of SRP concentrations on the rate and extent of P coprecipitation, are being pursued in our second experiment where a longer incubation period (3 months), using flow-through systems, is being utilized.

In October 2000, we initiated the second experiment for investigating the effects of Ca, alkalinity and SRP concentrations on P coprecipitation within SAV beds.

Tap water from the City of West Palm Beach was selected as the experimental source water because of its consistently low Ca (30 mg/L) and alkalinity (56 mg CaCO₃/L) concentrations relative to the 71 mg Ca/L and 227 mg CaCO₃/L alkalinity measured in Post-BMP agricultural drainage waters (ADW). We chose to add salts to the tap water to reach the desired alkalinity (375 mg CaCO₃/L) and Ca (100 mg Ca/L) concentrations rather than attempt to chemically remove them from the Post-BMP ADW. Opting for chemical removal would alter the water chemistry to such a degree that it would invalidate any comparison between low Ca/alkalinity (chemically “softened”) and untreated high Ca/alkalinity waters.

Because the West Palm Beach tap water has a chlorine residual and varying concentrations of SRP, dechlorination and SRP stripping were found to be necessary pre-treatment steps. This was accomplished by placing water hyacinths (*Eichhornia crassipes*) in the tap water reservoir for seven days. After the seven-day contact with water hyacinths, the water was pumped in 151L batches to four 208-liter holding reservoirs (Figure 1). The following Ca, alkalinity, and SRP amendments were added to each of the reservoirs:

Reservoir #1 (low Ca/alk and low SRP) – unamended

Reservoir #2 (low Ca/alk and high SRP) – amended with phosphate salts to yield final concentrations of 150 µg SRP/L

Reservoir #3 (high Ca/alk and low SRP) – amended with Ca and alkalinity salts to yield final concentrations of 100 mg Ca/L and 375 mg CaCO₃/L

Reservoir #4 (high Ca/alk and high SRP) – amended with Ca and alkalinity and phosphate salts to yield final concentrations of 100 mg Ca/L, 375 mg CaCO₃/L, and 150 µg SRP/L

In addition to the Ca, alkalinity, and SRP amendments, all the barrels received inorganic N, potassium, and micronutrient supplements (**Table 1**). After adding the nutrient amendments, the content of each barrel was pumped to duplicate 75-liter microcosms (Figure 1). Each of the eight microcosms (duplicates x 4 treatments) was initially stocked with 800 g (fresh wt) of *Najas guadalupensis*. No sediment was added to the microcosms.

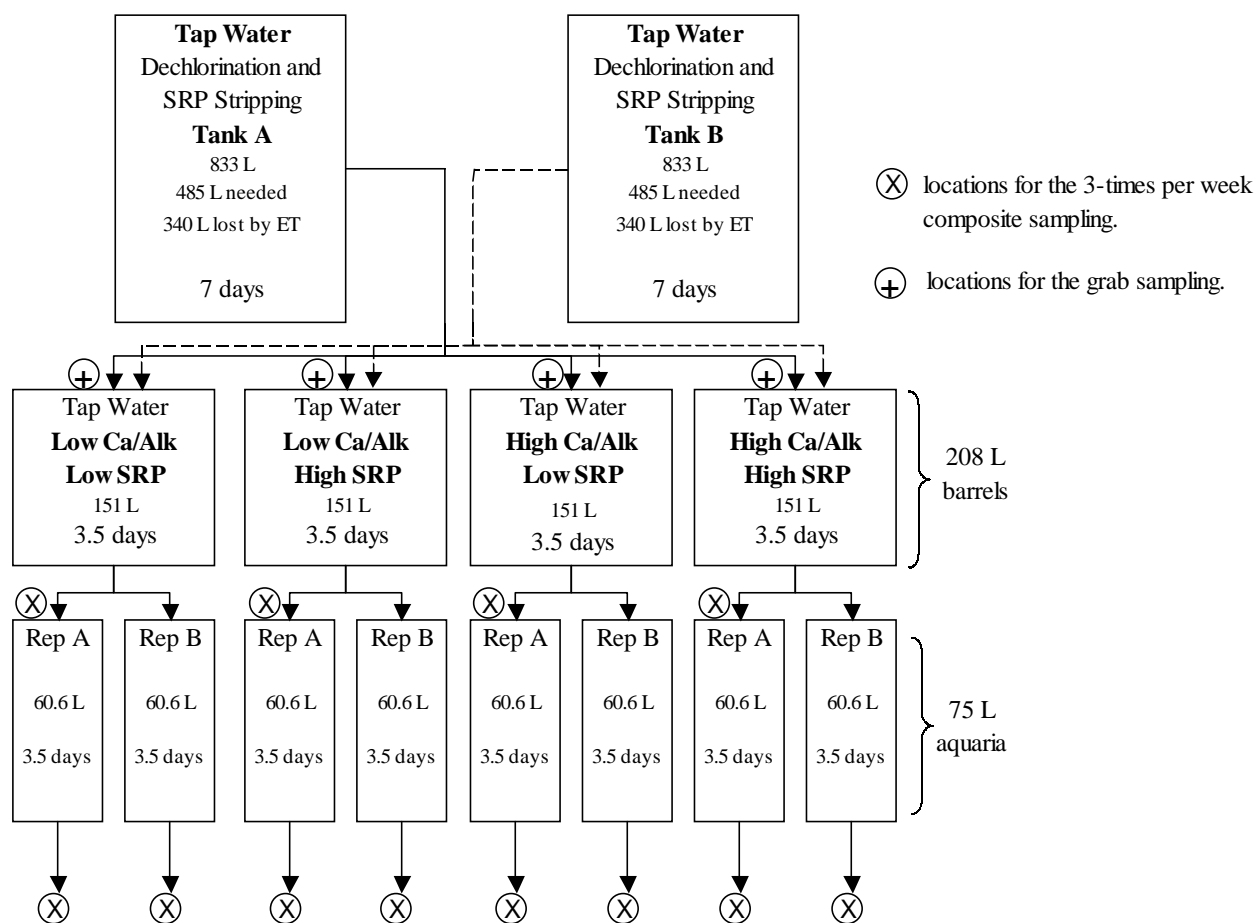


Figure 1. Flow chart detailing the experimental design for the flow-through Coprecipitation Experiment.

Table 1. Final concentration of nutrients and micronutrients amended to W. Palm Beach tap water.

Compound	Nutrient	Final Concentration
KCl	K ⁺	10.8 mg/L *
NH ₄ Cl	NH ₄ ⁺	0.5 mg N/L
KNO ₃	NO ₃ ⁻	0.5 mg N/L
H ₃ BO ₃	B	10.8 µg/L
MnSO ₄ ·H ₂ O	Mn	10.8 µg/L
ZnSO ₄ ·7H ₂ O	Zn	5.2 µg/L
CuSO ₄ ·5H ₂ O	Cu	1.2 µg/L
(NH ₄) ₆ Mo ₇ O ₂₄ ·7H ₂ O	Mo	0.4 µg/L
FeCl ₃ ·6H ₂ O	Fe (in EDTA)	16 µg/L
Na ₂ EDTA	EDTA	94 µg/L
Cyanocobalamin	B-12	3 µg/L

* 9.4 mg/L from KCl and 1.4 mg/L from KNO₃

A flow rate of 12 mL/min (17.3 L/day) was provided to each of the microcosms, which contained 60.6 L (16 gal) of water. This produced a HRT of 3.5 days (HLR=9.6 cm/day).

A composite of three grabs per week were collected at each sampling location (Figure 1) for TP, SRP, TSP, Ca, alkalinity, and conductance measurements. In addition to the composite sampling, we also collected grab samples after each time a new batch of source water was amended and stored within the holding tanks (Figure 1). Water temperature and pH measurements were taken in the field for each. Data from this study will be presented in subsequent monthly/quarterly reports.

Variable Depth Mesocosms (Subtask 5ii)

The fluctuating water depth experiment at the North Advanced Treatment Technology (NATT) site was initiated May 1, 2000 with a reduction of the water depth to 0.8 m in duplicate deep (1.2 m) mesocosms (referred to as “deep” mesocosms). Additionally, the water depth in two shallow (0.4 m) mesocosms (referred to as “shallow” mesocosms) was increased to 0.8 m. These depths were maintained for 5 weeks, after which time the shallow and deep mesocosms were returned to their original depths of 0.4 m and 1.2 m, respectively. During the subsequent 4 months, the depth fluctuations were imposed every five weeks, providing varying water depths between 0.4 and 0.8 m for the shallow mesocosms, and between 0.8 and 1.2 for the deep mesocosms. The process of raising and lowering water depths was performed gradually over a four-day period. Beginning at the end of September, we lowered the water level in the shallow and deep depth mesocosms to 0.15 and 0.40 m deep, respectively. After five weeks at these lower than normal depths, the water level in each of the four mesocosms was returned to its previous stage of either 0.4 or 1.2 m for three final weeks. During the entire study, one of each of the shallow and deep mesocosms, and all of the three moderate depth (0.8 m) mesocosms from previous Static Depth experiments, were held at a constant depth to serve as “controls” (i.e., non-fluctuating depth). The nine mesocosms in this experiment were sampled for total P and SRP weekly.

No substantial differences in the outflow TP concentrations were observed between either variable depth treatments, or between static and variable depth mesocosms, during the first 16 weeks of operation (Figure 2). However, in August 2000, differences developed between the

outflow TP concentrations from the static and those from the variable shallow depth mesocosms. The outflow quality from the variable depth mesocosms at this time did not appear to be impaired by a further depth reduction to 0.15 m (Figure 3), even though we observed some desiccation of the top portion of the SAV (*Chara*) standing crop.

The deep mesocosms, when lowered to a depth of 0.4 m, did not exhibit elevated outflow TP concentrations when compared to previous varying water depth cycles, or to the 1.2 m static “control” mesocosm (Figure 3). However, an increase in their outflow TP concentrations relative to the static “control” mesocosms was observed for the subsequent 3-week period when water depth was returned to 1.2 m (Figure 3). The most obvious explanation for the export of TP from the variable deep mesocosms after the increase from 0.4 to 1.2 m water depths is that inflow water was routed over the top of the “shortened” SAV canopy.

Mesocosms for Long-Term Monitoring (Subtask 5iv)

Three NATT site mesocosms have been operated since June 1998 at separate, constant hydraulic loading rates (HLR), water depths and hydraulic retention times (HRT). The relative performance of these treatment units has been fairly uniform over the long term (Figures 4 and 5). During the August-October 2000 quarter, outflow TP concentrations from mesocosms with an HRT of 1.5, 3.5 or 7.0 days averaged 51, 44, and 35 µg/L, respectively. The 1.5-day retention time produced similar outflow concentrations during the quarter vs. the entire period of record (POR) of 26 months (53 µgTP/L), while the longer HRT mesocosms exhibited higher outflow concentrations over the last three months than during the complete POR (3.5-day HRT for POR: 32 µg TP/L; 7.0-day HRT for POR: 26 µg TP/L).

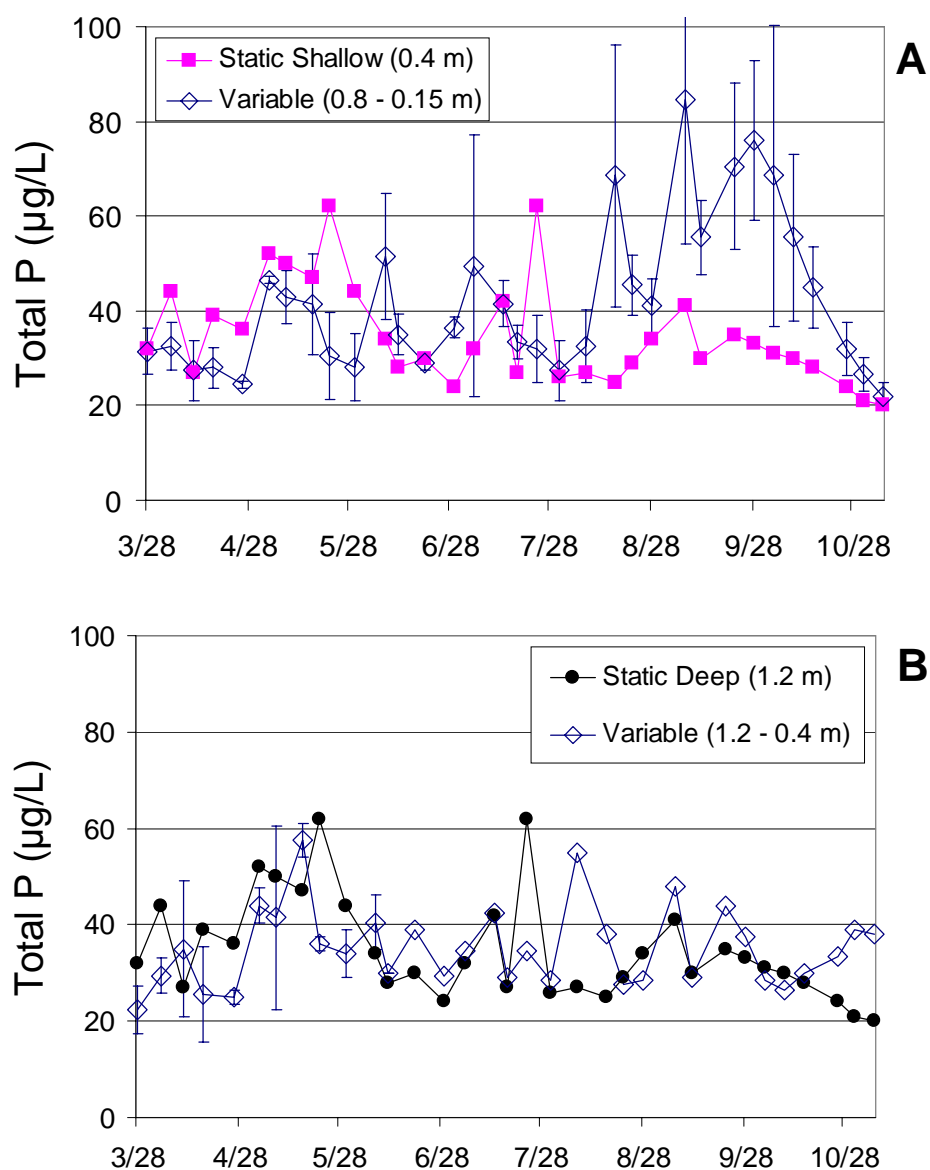


Figure 2. Total P outflow concentration for static and variable depth shallow mesocosms (A) and static and variable depth deep mesocosms (B).

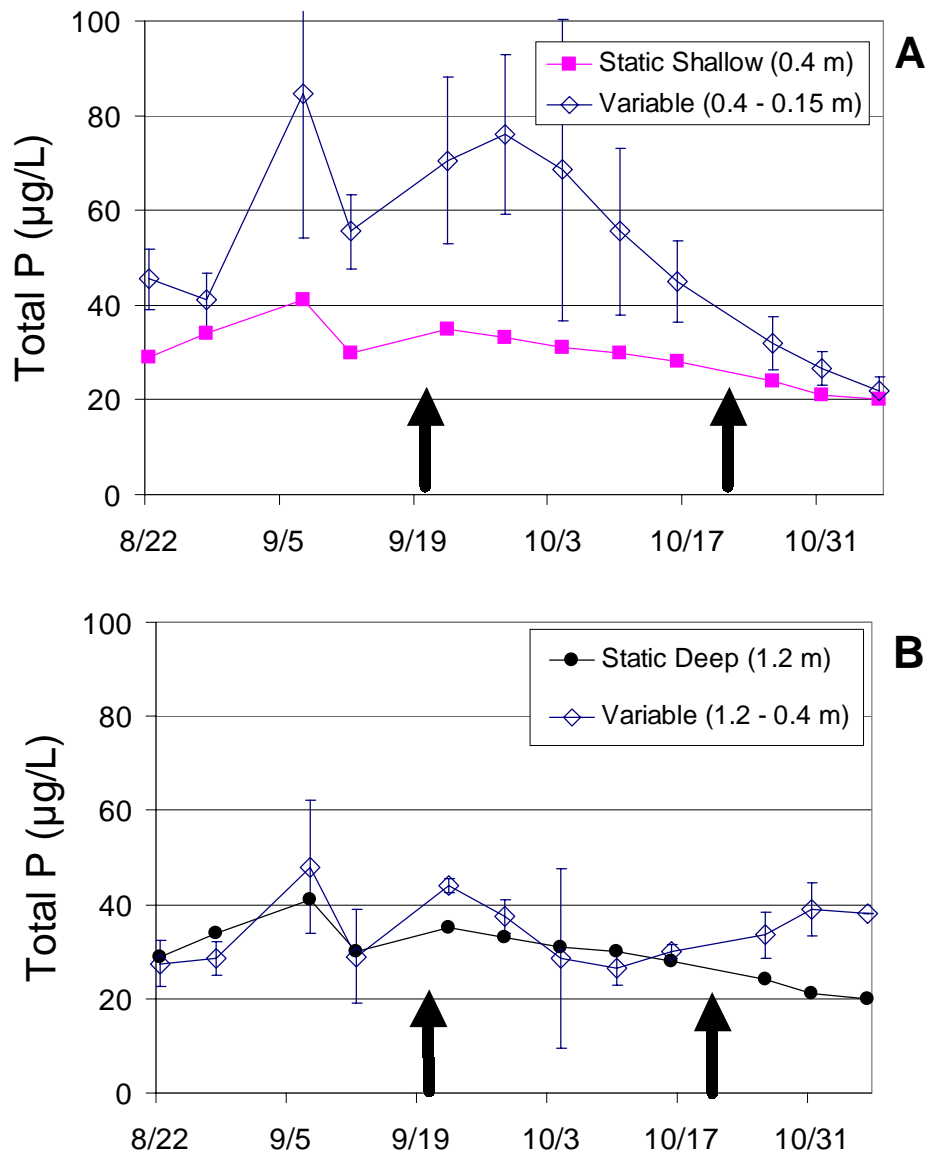


Figure 3. Total P outflow concentrations for static and variable depth mesocosms during final two months of study. Interval between arrows represents depth reduction to 0.15 m for shallow tanks (A), and to 0.4 m for deep tanks (B).

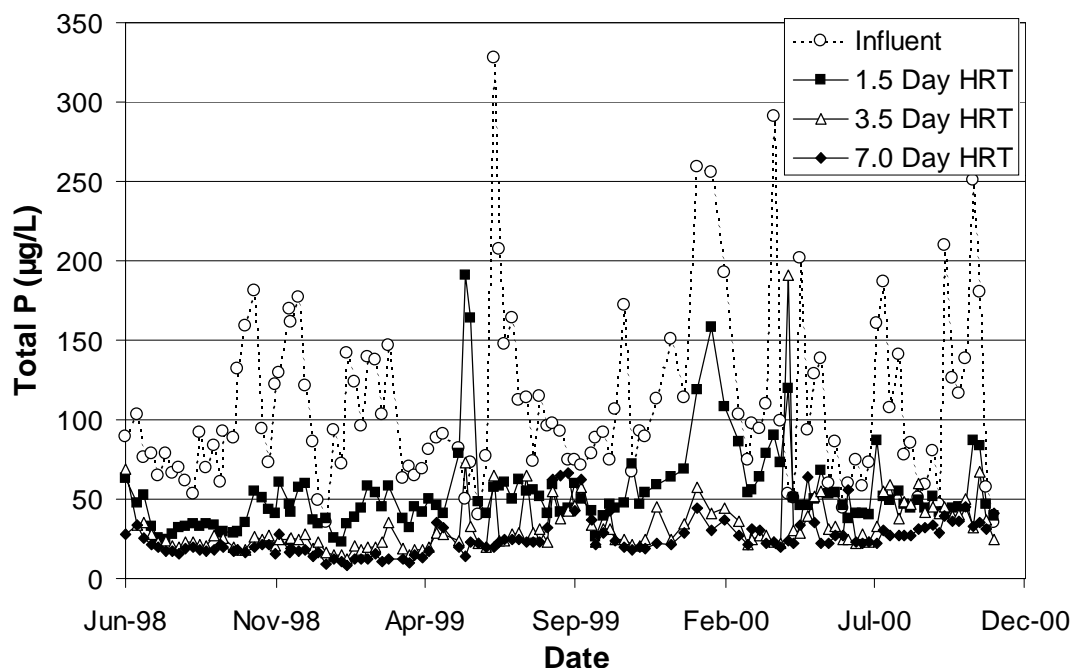


Figure 4. Inflow and outflow total P concentrations for mesocosms receiving Post-BMP waters at HLRs of 11, 22 and 53 cm/day (7.0-, 3.5- and 1.5-day HRTs). An expanded view of outflow concentrations is provided in Figure 5.

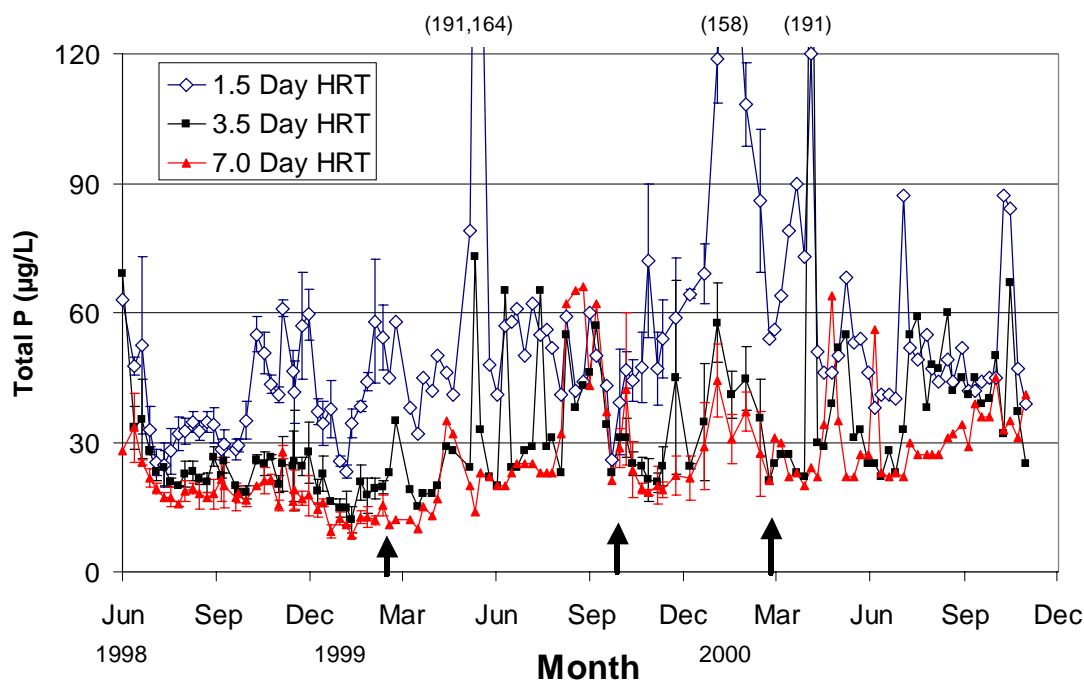


Figure 5. Outflow total P concentrations (mean, \pm 1 s.d) from mesocosms receiving Post-BMP waters at HLRs at 11, 22 and 53 cm/day (7.0- 3.5-, and 1.5-day HRTs). Single mesocosms were sampled during the time intervals between the first two arrows and after the third arrow; triplicate mesocosms were sampled during the other periods.

The Effects of Pulse Loading and Drydown/Reflooding on P Removal Performance (Subtask 5v)

Pulsed Loading

The six pulsed loading mesocosms continued to receive loadings according to the schedule based on the STA-2 data set (Table 2). During the August-October 2000 quarter, the hydraulic loading rates (HLRs) ranged from 0-400% of annual mean flow. These broad fluctuations reflect variable flows associated with “typical” wet season pumping events and periods of “no flow” during the dry season.

Table 2. Forty-week (Feb. 20 - Nov. 24, 2000) pulse loading schedule for low, medium, and high loaded mesocosms in Subtask 5v. The shaded section of the table correspond to the current reporting quarter.

Loading schedule (cm/day)				Loading schedule (cm/day)			
Week	Low	Medium	High	Week	Low	Medium	High
1*	0	0	0	21	13.2	26.4	66
2	0	0	0	22	13.2	26.4	66
3	22	44	110	23	44	88	220
4	22	44	110	24	44	88	220
5	4.4	8.8	22	25	0	0	0
6	4.4	8.8	22	26	0	0	0
7	0	0	0	27	26.4	52.8	132
8	0	0	0	28	26.4	52.8	132
9	13.2	26.4	66	29	8.8	17.6	44
10	13.2	26.4	66	30	8.8	17.6	44
11	0	0	0	31	35.2	70.4	176
12	0	0	0	32	35.2	70.4	176
13	0	0	0	33	6.6	13.2	33
14	0	0	0	34	6.6	13.2	33
15	26.4	52.8	132	35	11	22	55
16	26.4	52.8	132	36	11	22	55
17	0	0	0	37	22	44	110
18	0	0	0	38	22	44	110
19	17.6	35.2	88	39	0	0	0
20	17.6	35.2	88	40**	0	0	0

* Beginning week for Pulse Loading experiment: Feb. 20, 2000

** Expected week for terminating Pulse Loading experiment: Nov. 24, 2000

Low-, moderate- and high-load pulsed mesocosms were operated at HLRs of 44, 88, and 220 cm/day, respectively, during the two-week period of July 24 – August 7, 2000. These HLRs were the highest scheduled during the 40-week mesocosm study. They were followed by two

weeks of zero flow, which resulted in relatively high outflow TP concentrations for the month of August in the high and moderate flow treatments (Figure 6).

During the quarter, differences between the pulsed and constant flow mesocosm outflow TP concentrations were greatest in the high flow systems, and less in the moderate and low flow systems (Figure 7). These differences are typical for the entire POR through October (36 weeks); at the moderate and low loadings there was little difference between pulsed and constant flow treatment performances, but the highly loaded systems were subject to periods of poor performance (Figure 7 and Table 3). However, it should be noted that our maximum experimental HLRs (220 cm/day) are two orders of magnitude above the design mean flows for an STA [mean (max.) HLR = 2.3 (53) cm/day], and are not likely to be applied to a full scale SAV-based STA.

Table 3. Mean total phosphorus concentrations ($\mu\text{g/L}$) in the influent and outflows of pulsed and constant flow mesocosms receiving low, moderate and high loadings from February 21 – November 3, 2000.

	Influent	Outflow		
		High Load	Moderate Load	Low load
Pulsed	109 ^A	68 ^A	46 ^A	33 ^A
Constant	108 ^B	56 ^C	41 ^C	31 ^C

^A The mean of twice weekly sampling values in duplicate mesocosms.

^B The mean of weekly values from three mesocosms (low, moderate and high).

^C The mean of weekly values from a single mesocosm.

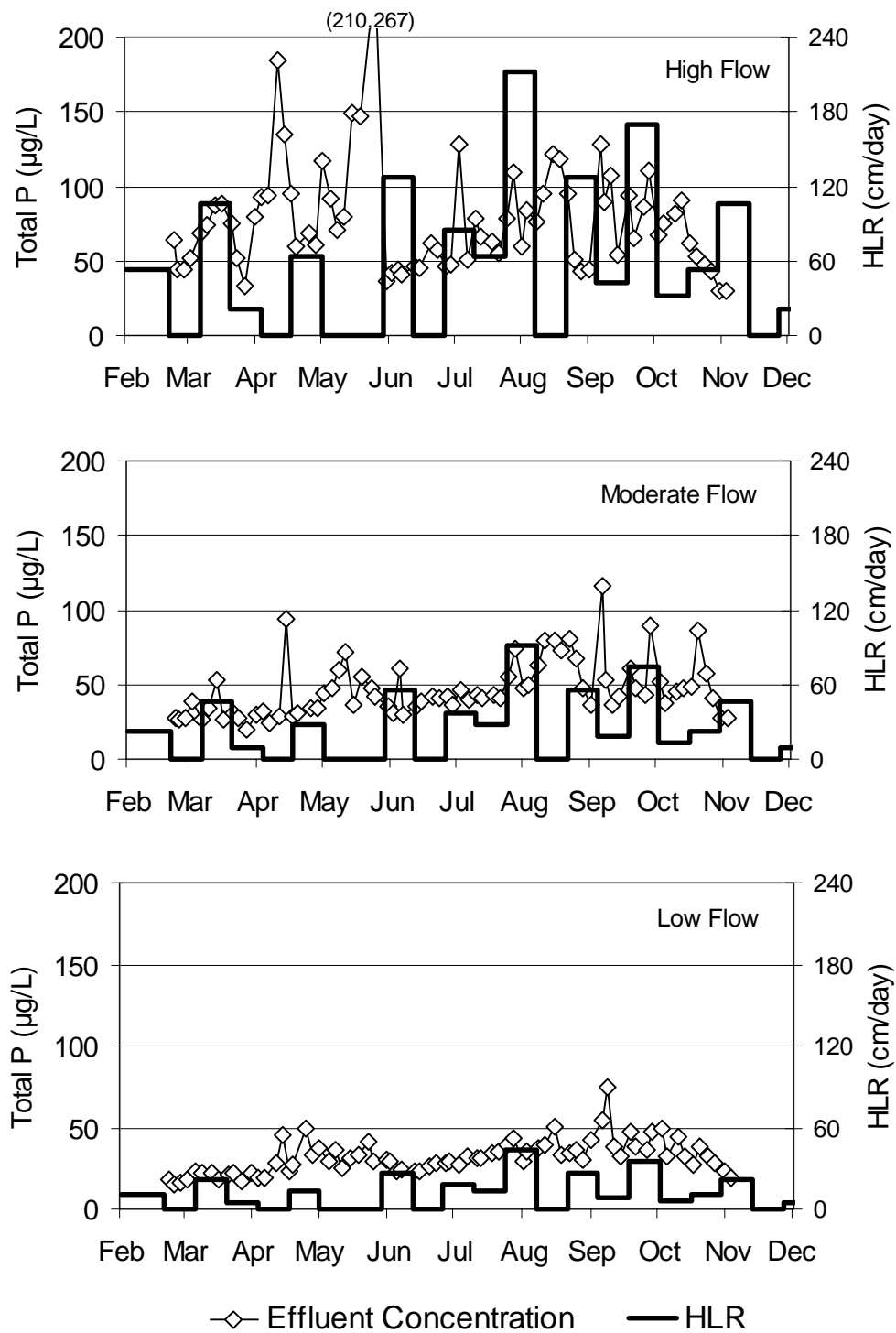


Figure 6. Mean outflow total P concentrations from mesocosms that received high, moderate and low pulse loading regimes.

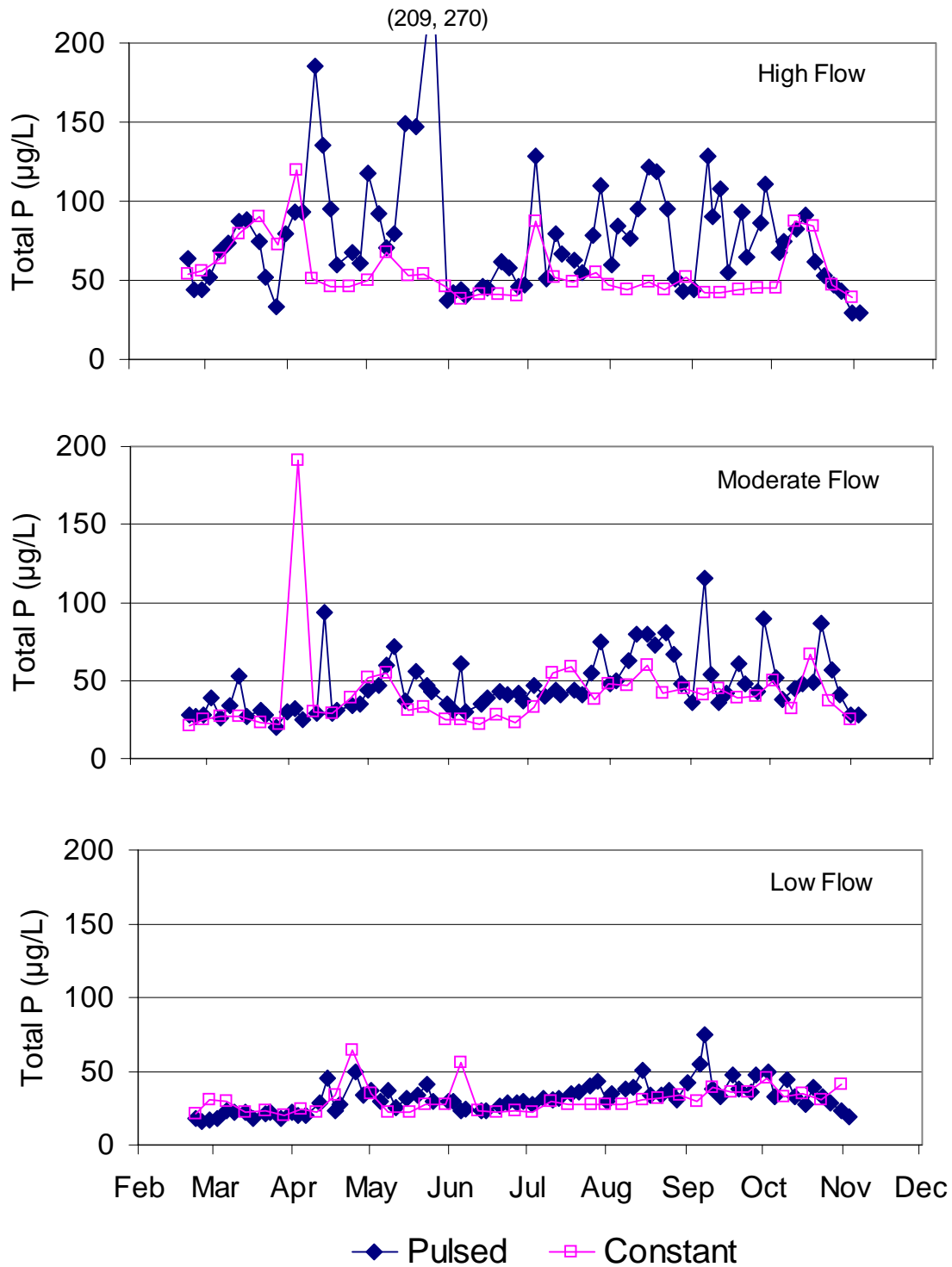


Figure 7. Outflow total P concentrations from mesocosms that received high, moderate and low flows of Post-BMP waters under pulsed and constant-flow regimes.

Sequential SAV/LR and Cattail Mesocosms (Subtask 5vi)

Sequential SAV/LR Mesocosms

We reconfigured the sequential treatment train in late July, adding a limerock barrel between the initial, deeper mesocosm, and the subsequent shallow mesocosm (see DBEL 2000). Additionally, we removed ~ 0.3 m of muck substrate from the shallow mesocosm to normalize the substrate thickness to ~ 0.2 m for both mesocosms in the system. We also increased the water depth from 0.4 m to 0.6 m. Subsequently, *Najas* was inoculated into the shallow (now 0.6 m deep) mesocosms. We interrupted our bi-weekly TP monitoring of the shallow mesocosm and LR outflows to allow the *Najas* inoculum to acclimate. Beginning in November, we will resume biweekly sampling for TP in both intermediate and final LR outflows, and in the shallow mesocosm outflows.

Phosphorus Removal Efficiencies within Cattail- and SAV-Dominated Mesocosms

Wetlands dominated by emergent macrophytes such as cattails may function differently than wetlands dominated by SAV, since SAV can enhance both photosynthesis and nutrient uptake within the water column. An increase in water column photosynthesis leads to an increase in daytime pH, which in turn can result in a chemical immobilization of P in hard waters by coprecipitation with calcium carbonate. As part of this study, we are testing the hypothesis that P removal is more efficient in a SAV community than in a cattail community when the inflow waters have high hardness concentrations.

Beginning in mid-February 2000, we resumed synoptic sampling of the influent and outflow waters (one grab from each location) of the two cattail and three shallow depth SAV mesocosms. In order to make comparisons between the relative P removal efficiencies as valid as possible, we selected mesocosms representing the two types of plant communities which had equivalent water column depths (0.4 m), HLRs (10 cm/day), and HRTs (3.6 days). Weekly grab samples from both sets of mesocosms were composited over a two-week period before being analyzed for SRP, TSP, TP, alkalinity, and calcium levels. The number of replicate shallow depth SAV mesocosms was reduced from 3 to 1 on March 28, 2000, which was the date when SD-1 and SD-3 mesocosms were subjected to fluctuating water depths under Subtask 5ii. Thus

only the SD-2 mesocosm, which served as a "depth" control (constant water depth maintained at 0.4 m), was used in the comparison with the cattail mesocosms.

A comparison of the total P concentrations in the outflows of the cattail and SAV mesocosms indicates a consistent pattern of superior P removal by SAV since January 1999 (Figure 8). We ascribe the difference in P removals to more underwater photosynthetic activity in the SAV community than in the emergent *Typha* community. Besides shifting the pH to higher (and more towards CaCO_3 supersaturation) values, the SAV species can also directly take up water column P because of their submerged habit.

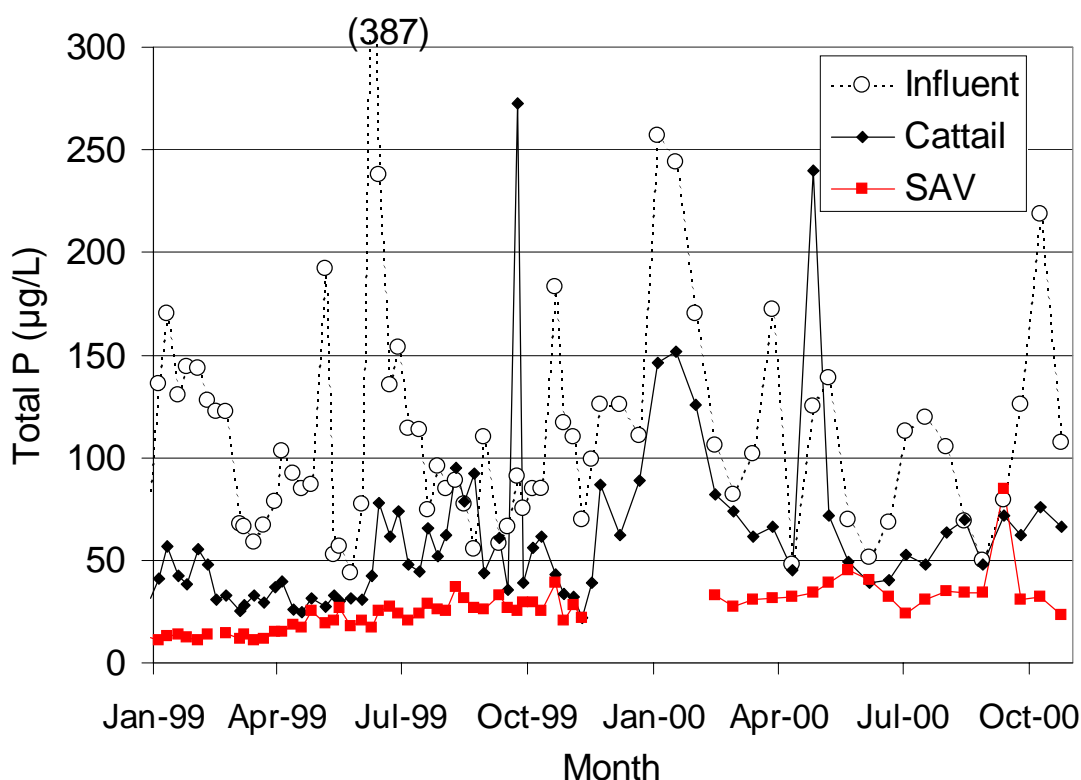


Figure 8. Total P concentrations in the outflows of shallow (0.4 – 0.5 m depth) mesocosms dominated by cattail and SAV communities. The number of replicate SAV mesocosms was reduced from three to one on March 28, 2000. Sampling suspended in the SAV mesocosms between November 9, 1999 and February 2000 because of biomass harvesting.

The quarterly data indicate that the P removal efficiencies for all three P fractions (SRP, TSP, and TP) were higher for the SAV mesocosm than either of the two replicate cattail mesocosms

(Table 4). In addition, the pH was higher and the alkalinity concentration reductions were greater in the SAV community than in the cattails, suggesting that more calcium carbonate precipitation was occurring within the SAV system. Although more data are needed before definite conclusions can be drawn regarding the relative P removal efficiencies of cattail and SAV communities, it appears from this data set that SAV wetlands exhibit superior P removal processes.

Table 4. Comparisons between one SAV- and two cattail-dominated mesocosms at the NATT site in the removal of SRP, TSP, TP and alkalinity during the August – October 2000 period of record. The inflow values represents the average of samples collected from one of the cattail mesocosms and the SAV mesocosm.

Station	pH	SRP (µg/L)	TSP (µg/L)	TP (µg/L)	Alk (mg CaCO ₃ /L)	Sp Cond (µmho/cm)
Inflow	7.81	68	86	108	169	1148
Cattail Outflow						
Rep 1	8.02	26	47	71	274	1148
Rep 2	8.03	12	26	59	279	1155
SAV Outflow	9.09	3	16	39	169	969

Shallow, Low Velocity SAV/Periphyton/Limerock Systems (Subtask 5vii)

During the August–October quarter, the shallow (0.09 m depth) SAV/periphyton raceways at the SATT site continued to perform well, having fully recovered from the period of high inflow TP concentrations during April and May. During this quarter, the outflow from the final limerock beds was 10 µg/L or less for 7 of 13 weekly grab samples (Figure 9). Influent concentrations for the same period averaged 24 µg TP/L. These shallow systems have received an HLR of 22 cm/day since May 2000, with an average HRT of 0.4 days. The experiment is scheduled to be terminated late in November 2000 to allow the platform to be reconfigured for velocity experiments.

Growth of SAV in Post-STA Waters on Muck, Limerock, and Sand Substrates (Subtask 5ix)

In an effort to understand the interaction between HLR and different substrates on P-removal performance by SAV, we reduced the HLR to the sand, muck, and limerock substrate mesocosms on several occasions during the past six months (Figure 10). On three occasions

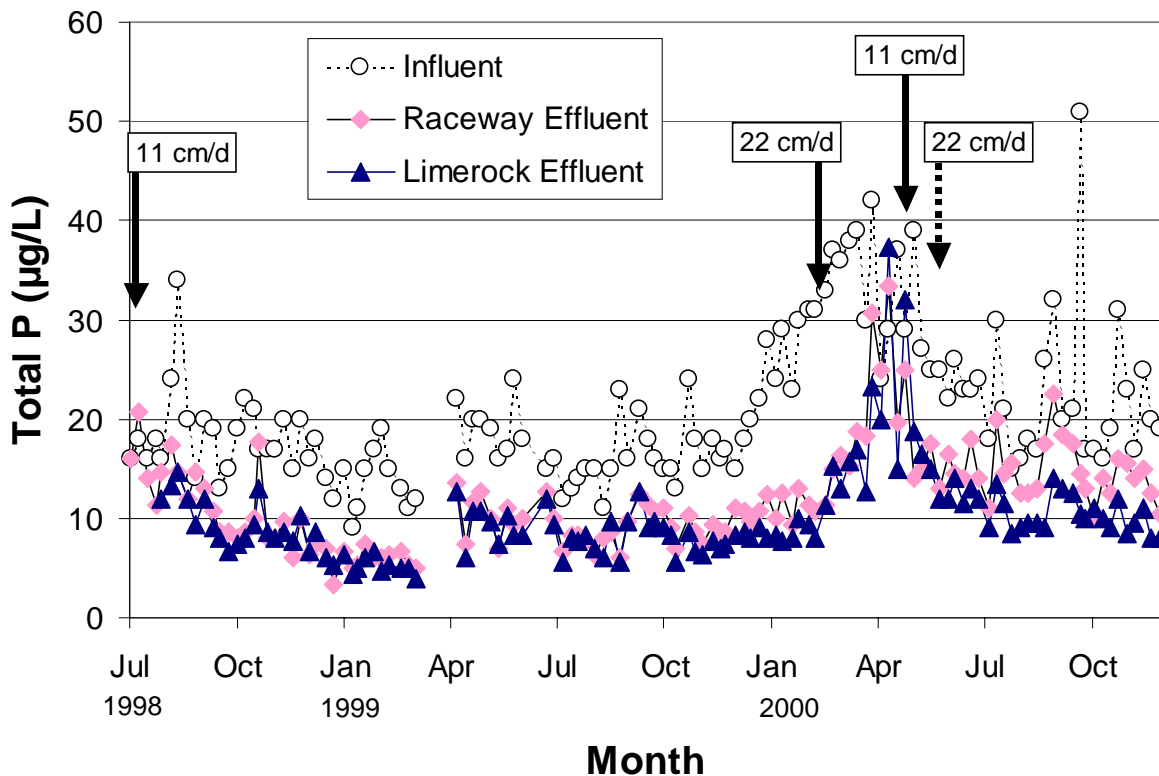


Figure 9. Total P concentrations in the influent and outflows of triplicate shallow, low velocity, SAV/periphyton raceways, and in the outflow of the subsequent limerock beds. Dates of flow manipulations are depicted on the figure. Values after the dashed arrow represent means of duplicate raceways.

during the February-May period, the flows were reduced by 50%. Each treatment train is now being operated at a 7.5 cm/day HLR.

During this fourth quarter, mean system outflow TP concentrations were lower from the limerock (12 µg/L) than the muck (14 µg/L); sand exhibited the highest outflow TP (21 µg/L) (Table 5). This is contrary to trends described in earlier reports (DBEL 2000), where the muck substrate mesocosms provided lowest outflow TP concentrations (Figure 10). Although the SAV biomass is sparse in the limerock substrate mesocosms, they recently have performed as well as (or better than) the muck substrate mesocosms, which do support dense SAV populations. Clearly, removal mechanisms other than SAV uptake are occurring within the mesocosms. These mechanisms may include microbial uptake (bacterial and nanoplankton), enzymatic P hydrolysis, adsorption, photolysis and particle P sedimentation. Moreover, the limerock substrate may perform a role important for P removal by maintaining alkalinity levels in the

water column (P coprecipitation with CaCO_3) or by creating an environment amenable to refractory sediment-P accretion.

Table 5. Mean total phosphorus concentrations (± 1 standard deviation) in the influent and outflows of duplicate substrate mesocosms during August - October 2000.

	Influent	Limerock	Muck	Sand
Mean ($\mu\text{g/L}$)	19 ± 1	12 ± 1	14 ± 2	21 ± 5
Max ($\mu\text{g/L}$)	31	16	20	35
Min ($\mu\text{g/L}$)	15	9	9	11

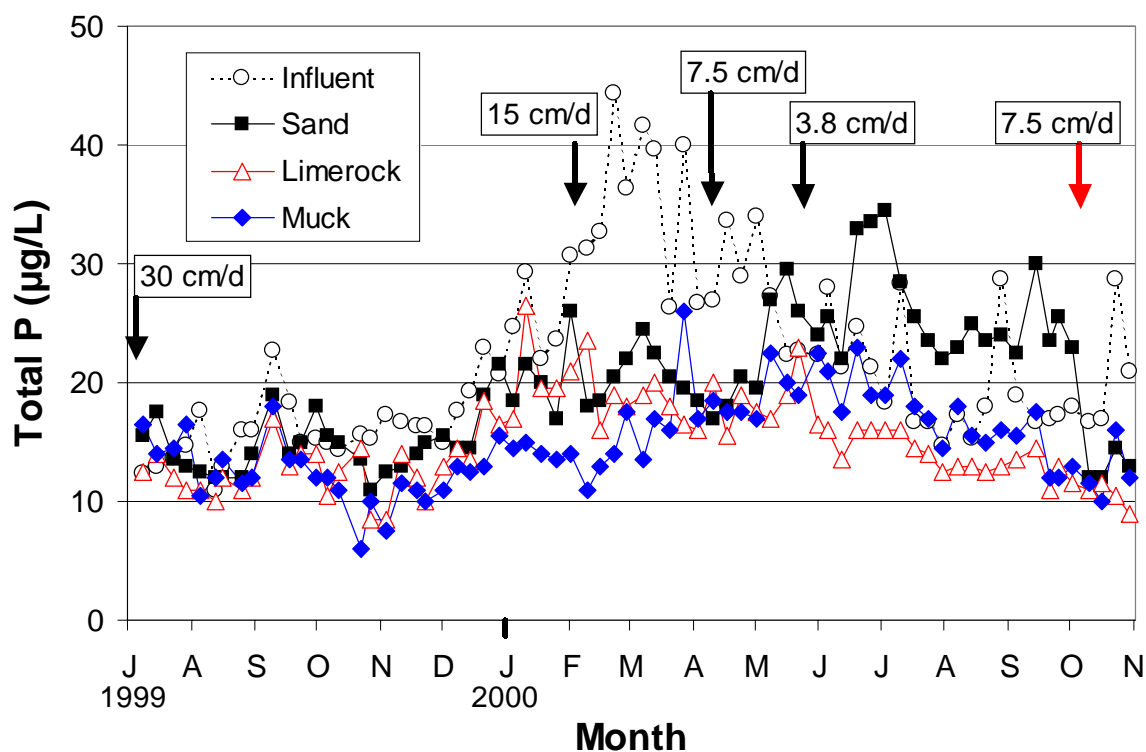


Figure 10. Total Phosphorus concentrations in the influent ($n = 3$) and outflows ($n = 2$) of SAV mesocosms established on limerock, muck and sand substrates.

The Effects of Filter Media Type and Size on P Removal Performance (Subtask 5x)

Our initial work with the SAV/LR concept at the North and South Advanced Treatment Technology sites demonstrated that a LR bed serves principally as a physical filter for particulate P. During August, sixteen small, outdoor filter columns were constructed at the South Advanced Treatment Technology (SATT) site. The columns contained one of four different filter media types within various size ranges (Table 6).

Table 6. Filter media types and particle sizes used in the Filter Media Experiment (Subtask 5x).

Sieve No.	Size Range	Filter Media Type			
		Quartz Sand	Limerock	Pro-Sil Plus™ [†]	Fe-coated Sand
<No. 3	Coarse 3.35-6.86 mm	✓	✓	✓	
>No. 6					
<No. 6	Medium 2.00-3.35 mm	✓	✓	✓	
>No. 10					
<No. 20	Fine 0.25-0.85 mm	✓			✓
>No. 60					

[†] A combination of Ca and Mg silicates.

In this experiment, Post-STA (low soluble reactive and particulate P) waters are pumped to three supply tanks (4.66m long x 0.79m wide x 1.00m deep) containing SAV and then gravity-fed through PVC columns (20.3 cm ID), with 56 cm depth of packed medium, providing a hydraulic retention time of 91-131 min. Support for the filter medium within each column consists of layers of glass wool and pea gravel (Figure 11). This prevents the loss of the fine-grained media in the column outflow.

Sampling of the column influents and outflows was performed from August 18 to November 17, 2000. Total, total soluble, and soluble reactive phosphorus concentrations were analyzed as twice-weekly grab samples, while specific conductance, calcium and alkalinity samples were composited each week. Mean influent and outflow concentrations of TP, SRP, Ca and alkalinity are presented in Table 7. Outflow TP concentrations were similar among treatments (13 – 15 µg/L) except for the fine-grained quartz (sand) and iron-coated sand, both of which exported P. The medium-grain Pro-Sil Plus media provided the lowest mean outflow TP concentration (13 µg/L) of any treatment during the first ten weeks of operations.

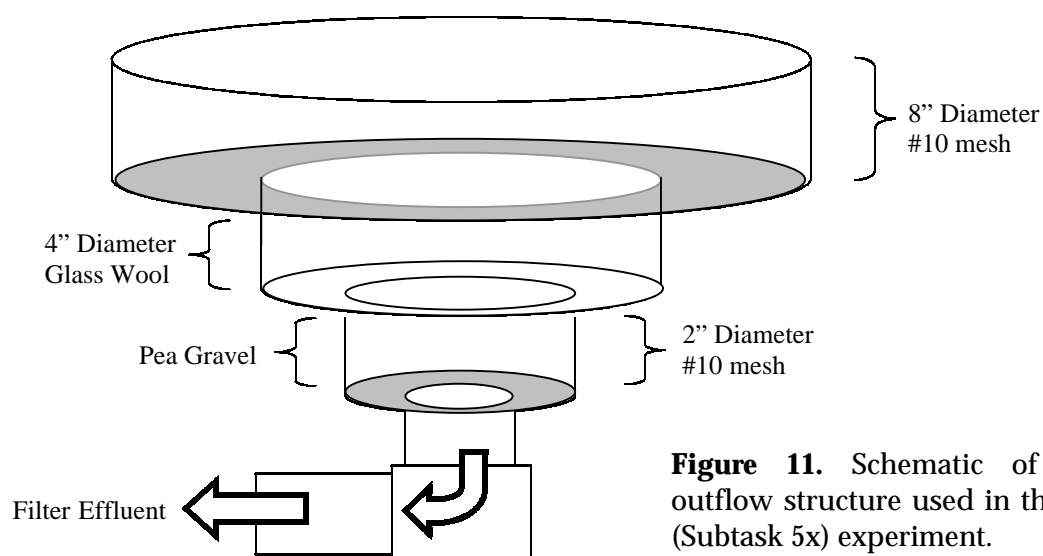


Figure 11. Schematic of the column outflow structure used in the Filter Media (Subtask 5x) experiment.

The Pro-Sil Plus™ media also reduced calcium and alkalinity concentrations by 16%, whereas for other media types these constituents increased or remained unchanged (Table 7). The iron-coated sand columns have released large quantities of SRP since flow was initiated (Figure 12), and although the release rate has decreased since startup, we discontinued weekly sampling of this filter media type until the last week of the 3-month study.

Table 7. Mean (± 1 s.d.) TP, SRP, calcium and alkalinity concentrations in the influent and outflows of the Filter Media experiment (Subtask 5x) during the August 18-October 30, 2000 period of record.

	Influent	Quartz			Limerock		Pro-Sil Plus™		Iron-coated Sand
		Coarse	Med.	Fine	Coarse	Med.	Coarse	Med.	Fine
Total P ($\mu\text{g/L}$)	17 ± 4	15 ± 5	15 ± 4	18 ± 5	15 ± 4	14 ± 6	14 ± 4	13 ± 3	133 ± 74
SRP ($\mu\text{g/L}$)	3 ± 2	4 ± 3	4 ± 3	8 ± 2	3 ± 2	3 ± 1	3 ± 1	2 ± 1	96 ± 68
Calcium (mg/L)	73 ± 5	76 ± 6	76 ± 7	76 ± 5	76 ± 5	76 ± 6	69 ± 12	69 ± 12	73 ± 7
Alkalinity (mg CaCO_3/L)	250 ± 13	258 ± 14	258 ± 12	255 ± 15	256 ± 12	259 ± 12	238 ± 47	235 ± 51	259 ± 14

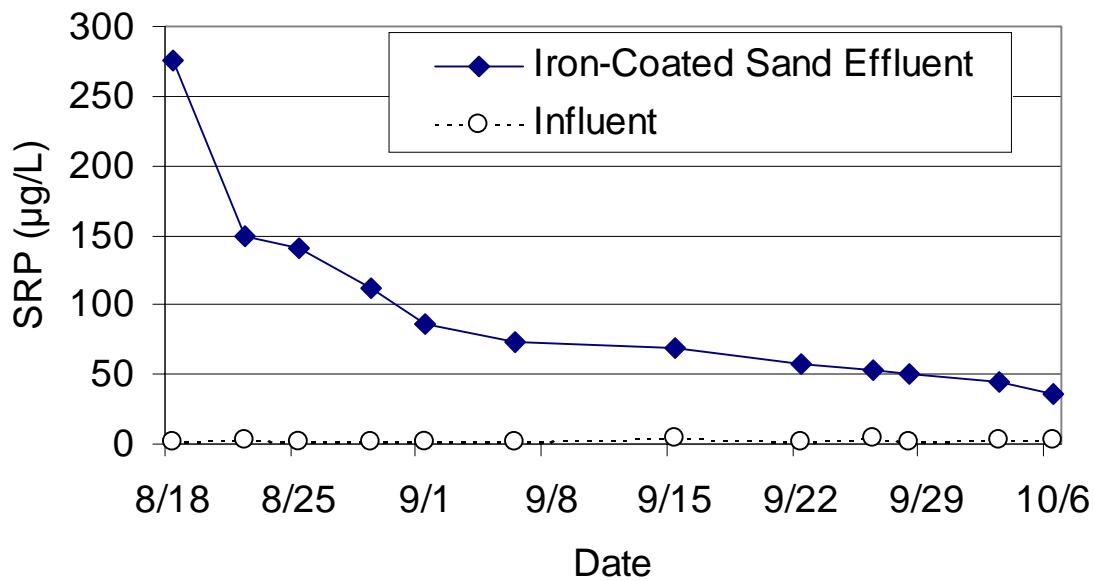


Figure 12. SRP release from the iron-coated sand filter column during Aug. 18-Oct 6, 2000.

References

DB Environmental (DBEL). 2000. A Demonstration of Submerged Aquatic Vegetation/Limerock Treatment System Technology for Removing Phosphorus from Everglades Agricultural Area Waters: Follow-on Study. Third Quarterly Reprt submitted to South Florida Water Management District and the Florida Department of Environmental Protection. West Palm Beach, FL.

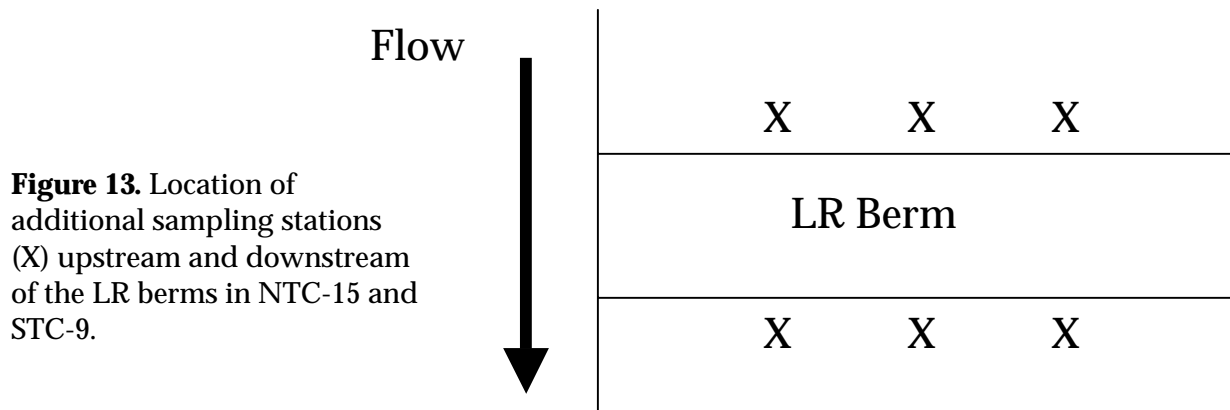
Task 6. Test Cell Investigations

Since September 11, 2000, the North SAV test cells have received a HLR of 11 cm/day and are being maintained at a water depth of 0.6 m. The water depth in the South test cells are held at a shallower depth (0.4 m), with an HLR of 5 cm/day. Each test cell's influent and outflow are composited (3 daily grabs/week) for analyses of TP, TSP, SRP, dissolved calcium, alkalinity, and specific conductance. Temperature and pH are measured with each sampling event.

Initial Performance of Test Cell Limerock Berms

In May 2000, limerock berms were constructed across the width of the cell in the outflow region of NTC-15 and STC-9 to provide particulate P filtration at the back end of the test cells. Results from mesocosm-scale experiments (Subtask 5iv) suggest that these berms will trap particulate P, which may ultimately transform to SRP. Any SRP released in this manner should be removed by the SAV located between the berm and the outflow weir. We have adjusted our sampling protocol accordingly, to record changes in SRP, PP, and DOP concentrations as water passes through the limerock berm.

During this quarter, we established additional sampling locations in NTC-15 and STC-9, the cells with the LR berms. These additional locations are located immediately upstream and downstream of the LR berm (Figure 13). The upstream (pre-berm) and downstream (post-berm) samples each represent a composite of grab samples from three locations. The samples, which are collected 3 days per week, are then composited weekly.



From August through October 2000, total P concentrations decreased 77% between the influent and outflow sampling locations in NTC-15 (Table 8). The concentrations of SRP dropped to near the detection limit (2 µg/L) before the LR berm. Particulate P concentrations increased from 11 µg/L after the berm to 13 µg/L at the outflow weir. Average SRP and DOP concentrations remained unchanged between the LR berm and the outflow weir (Table 8).

Table 8. Total, soluble reactive, dissolved organic, and particulate phosphorus concentrations (µg/L) at locations along the flow path in NTC-15 and STC-9 during the August – October 2000 quarter.

	Total P	SRP	DOP	PP
NTC-15				
Influent	100	39	16	47
Pre-berm	21	3	8	10
Post-berm	21	2	8	11
Outflow	23	2	8	13
STC-9				
Influent	23	5	9	10
Pre-berm	21	2	7	12
Post-berm	19	2	8	9
Outflow	17	3	6	8

The TP removal performance for NTC-1 and NTC-15 continued to improve throughout the August – October quarter, with outflow TP levels eventually declining to just above 10 µg/L (Figure 14). Doubling the flow rate to 11 cm/day in September did not affect the trend of declining outflow TP concentrations. There was little difference in the relative treatment performance of the two test cells, although outflow TP concentrations in NTC-1 were consistently lower than the outflow levels of NTC-15, which contained the LR berm.

In STC-9, the dissolved organic P (DOP) concentration declined by 33% between the influent manifold (9 µg/L) and the outflow weir (6 µg/L). The 5 µg/L average SRP level in the influent waters was reduced to near detection limits throughout the test cell. The limerock berm did

appear to provide some particulate P removal, which exhibited a concentration increase between the influent manifold (10 µg/L) and the pre-berm station (12 µg/L).

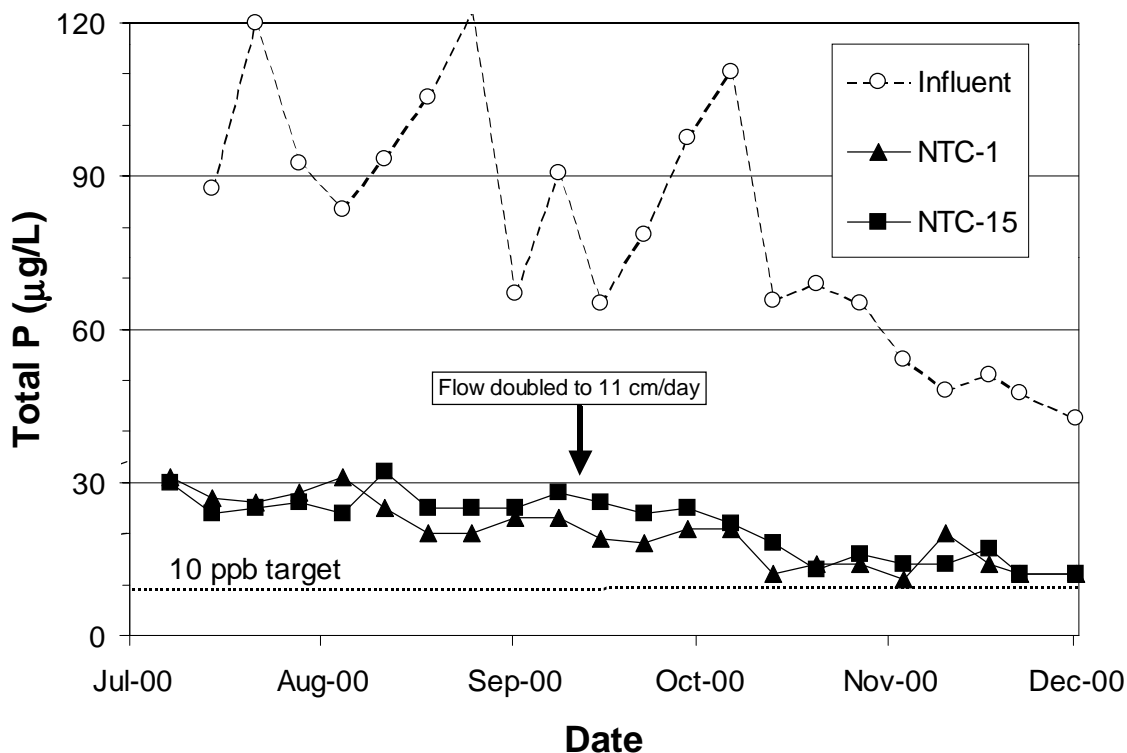


Figure 14. Total phosphorus concentrations in the influent and outflows of the North test cells during the August – October 2000 quarter.

For most of the August to October quarter, STC-4 and STC-9 provided only slight reductions in TP concentrations (Figure 15). However, the outflow TP concentrations in STC-9, which contains the LR berm, dropped to as low as 11 µg/L for the last two sampling events of the quarter.

Sediment Accretion Rates

To assist our future efforts in quantifying the accretion of sediments in the test cells, feldspar horizon markers were installed in each of the four SAV test cells (NTC-1, NTC-15, STC-4 and STC-9). We selected four stations within each test cell for placement of the feldspar marker locations - two were placed one-quarter distant from the inlet manifold (20 m) and about one-

third distant from each side bank, and two were located three-quarters distant from the inlet manifold (60 m), and again one-third from each side bank.

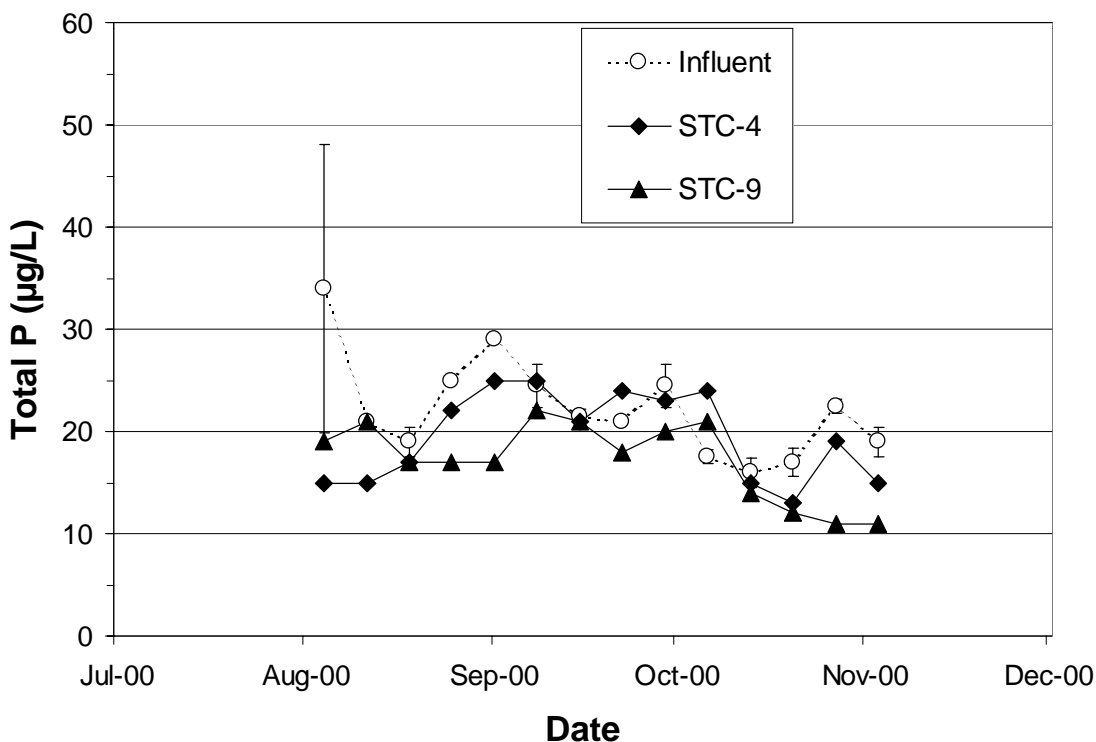


Figure 15. Total phosphorus concentrations in the influent and outflows of the South test cells during the August – October 2000 quarter.

At each of the four designated horizon marker locations within each test cell, we poured approximately 1.25 gallons of dry feldspar (potash of soda G-200) into a 43-cm diameter open-ended metal enclosure. This produced an initial horizon thickness of 3.3 cm. To allow enough time for the deposition of the feldspar, the metal enclosures were left in place for 24 hours after the initial pour. The location of each horizon marker was designated by four upright equally-spaced PVC poles arranged along the circumference of the feldspar layer. The area inside each of the horizon markers will be cored (4 cores per marker location) in May 2001 so that we can quantify sedimentation rates.

Task 9. STA-1W Cell 4 Performance Monitoring and Characterization

Intensive Water Quality Sampling

During our Cell 4 tracer study performed in December 1999, we conducted “internal” water column sampling for TP at numerous stations within the wetland. Flows and TP concentrations before, during, and after that sampling period were relatively constant (average inflow of 2.53×10^5 m³/day with an average TP concentration of 96 µg/L). In that study, we were able to demonstrate a relationship between P removal efficiency and the internal flow dynamics.

Since the tracer study demonstrated that short-circuited areas coincided with areas of reduced P removal efficiency, we presented several alternative structural changes within the footprint of Cell 4 to enhance P removal (DBEL 2000a). One of these recommendations, the construction of LR “plugs” perpendicular to the east and west levees where most of the short-circuiting occurred, was implemented by the District. Subsequent to the deployment of the LR “plugs”, and prior to the commencement of modifications to the transverse C-7 canal, we performed a second internal sampling within Cell 4. The major goal of this internal P survey was to evaluate the effects of the LR “plugs” on P removal and distribution, and to measure the P concentrations within what appeared to be newly established short-circuiting channels.

On August 9, 2000, we sampled surface water at 44 internal stations along 7 east-west transects and 1 north-south transect in Cell 4 (Figure 16). Temperature and pH were recorded in the field, and water samples were collected for SRP and TP analyses. Twenty-six of the 44 internal sampling stations coincided with the station locations of the previously sampled TP during the tracer study (DBEL 2000b). The 18 additional stations were selected to correspond to spatial gaps in the sampling grid that were recognized after our tracer study. For example, we added an additional transect at the northern-most boundary of the cell (Figure 16), which should better reflect the influent water quality. We have also included stations along a north-south short-circuit that recently developed along the western boundary. Besides the internal sampling, we also

composited inflows (August 8-10) and outflows (August 8-15, except for August 13) on a daily basis.

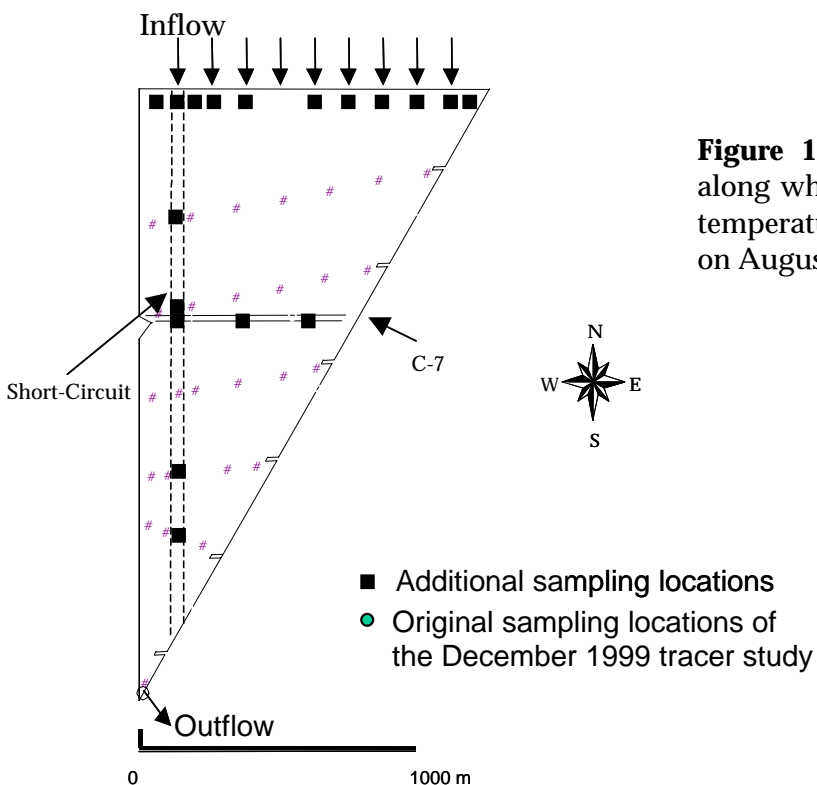


Figure 16. Internal transects in Cell 4 along which water quality (TP, SRP, pH, temperature) was evaluated at 44 stations on August 12, 2000.

Phosphorus concentrations varied considerably within the cell (Figure 17). As expected, TP and SRP concentrations were higher in the inflow region than in the rest of the cell. Areas of higher concentrations for both TP and SRP were found along the eastern and western levees of the cell, associated with short-circuited zones.

Short-circuiting was pronounced along the eastern side of the cell as well, but was confined to the northern half (Figure 17) of the wetland. We believe the flow along the eastern levee is diverted westward along the C-7 canal, where it resumes a southern course along the western levee.

Although the limerock plugs were partially successful in deflecting the flow path away from the western levee, they may have promoted a new short-circuit flow path to the east. This is suggested by the TP spatial concentration gradients in the western regions of Cell 4 before and

after installation of the limerock plugs (Figure 18). Therefore, during the second internal sampling of Cell 4, the flow was still unevenly distributed as new preferential flow paths were established following curtailment of the old ones by the structural modifications.

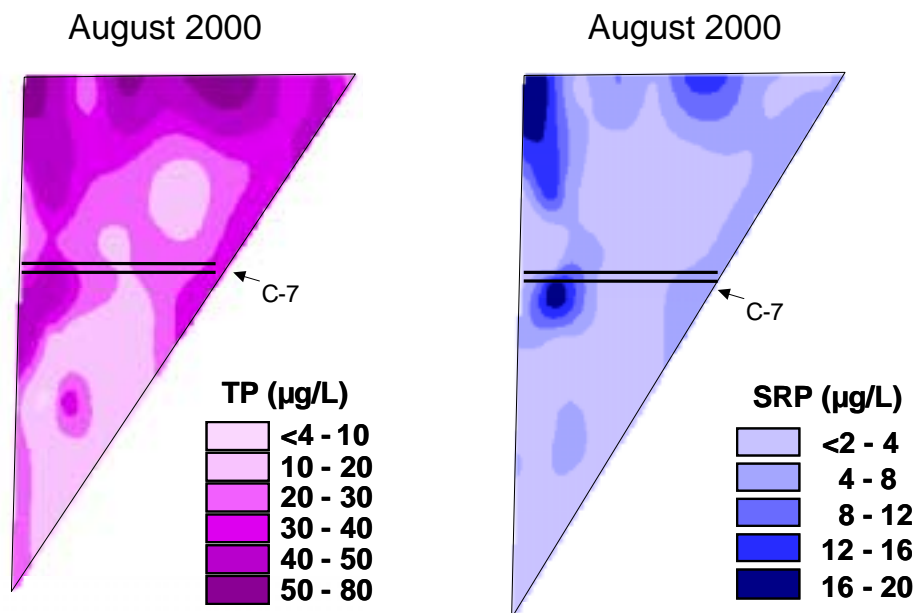


Figure 17. Total and soluble reactive phosphorus concentration gradients constructed from 44 stations internal to Cell 4 on August 9, 2000.

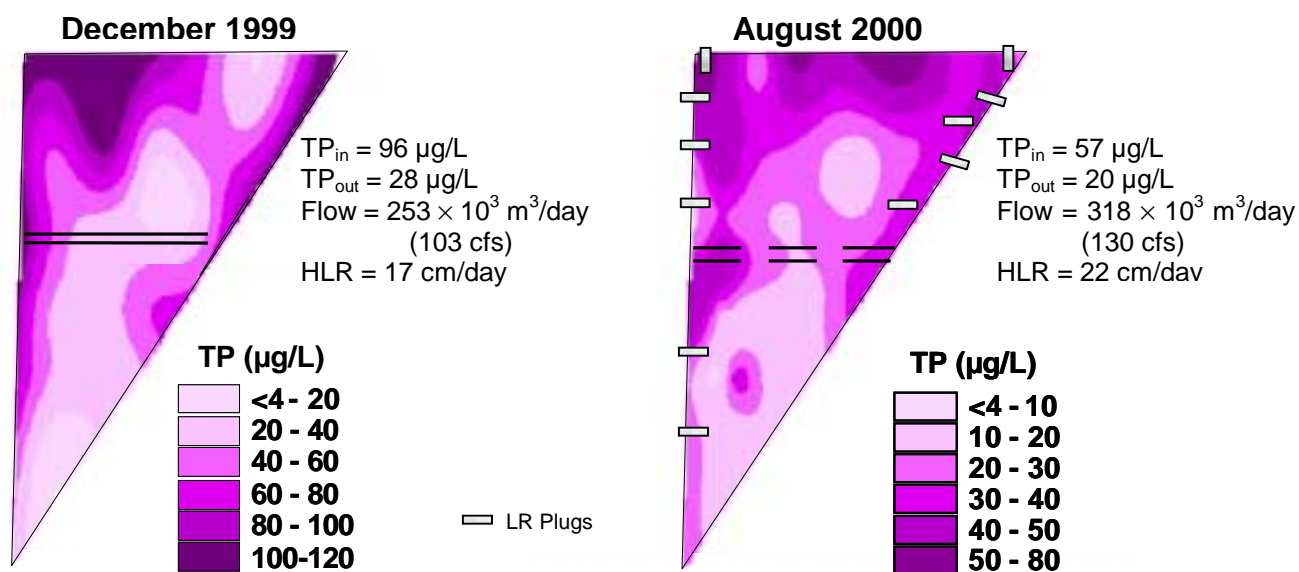


Figure 18. Spatial gradients in total P concentrations within Cell 4 before (sampled December 17, 1999) and after (sampled August 9, 2000) the addition of limerock “plugs”.

Sediment P Stability/Release Experiments

We initiated work on this task in June 2000, using sediments collected from the inflow region of Cell 4, and reported results from selected experiments (i.e., effects of pH and oxic vs. anoxic conditions on SRP release) in our Third Quarterly Report. Since that time, we have repeated the P-fractionation schemes and P stability/release treatments on sediments collected from the southern region (near the outfall) of Cell 4. Here we present the results of: a) the effects of pH and oxic vs. anoxic conditions on SRP release from Cell 4 outflow sediments; b) experimental treatments of desiccation followed by reflooding and; c) effects of high Ca, alkalinity, and SRP levels in the overlying waters, for both inflow and outflow sediments. Lastly, we compare characteristics of the extracted P pools for both inflow and outflow sediments.

Sediment Collection Methodology

We cored (10.1 cm ID aluminum corer) three stations along an east-west transect in the southern region of Cell 4 on July 18th. The calcium enriched accrued sediment (average 3-cm depth) deposited subsequent to flooding was separated from the underlying agricultural muck soil. One core from each station was kept separate for the fractionation analyses of the accrued sediment, while the accrued calcareous sediment in the remaining 10 to 12 cores from each station were composited and homogenized to provide substrate for the stability/release experiments. Additional extractions for P fractionation were performed on each composited sample. To prevent oxidation of the sediments during storage, nitrogen gas was injected into the headspace of the composite container and into the zip-lock bags holding the sediments for P fractionation.

Methodology for Sediment Stability Incubations

In this report, we describe methods and results for the following experiments with Cell 4 inflow and outflow sediments:

1. Desiccation followed by reflooding with atmospheric sparging
2. High Ca/Alkalinity levels with atmospheric sparging
3. High SRP levels (120 – 128 µg/L) with atmospheric sparging
4. Control (no desiccation or amendments) with atmospheric sparging

Incubations began on either June 15 (high Ca/alkalinity and oxic control) or June 19 (high SRP, reflow, and oxic control) with the composited inflow sediments, and on July 23 (all treatments and control) for the outflow sediments. The composited sediment samples were refrigerated under a blanket of nitrogen during the 1 to 5 days following field collection and prior to the incubations. Air (laboratory atmosphere) was sparged through distilled water prior to being gently bubbled (8 – 10 mL/min) into the water column of each incubation vessel. Incubations were performed in the dark, within a water bath held at room temperature. The minimum and maximum temperatures during the entire incubation periods (12.6 days) were 20 and 22°C for the inflow sediment incubation period and 19 and 23°C for the outflow sediment incubation.

Desiccation Followed by Reflooding

To assess effects of drydown and reflooding on sediment P release, we dried both Cell 4 inflow and outflow sediments in sunlight to achieve a partial desiccation. Following the partial desiccation outdoors, a subset of duplicate flasks for each sediment type was sacrificed by completely drying the sediment in an oven at 70 – 80°C so that the extent of the outdoor desiccation would be known.

Table 9 provides dry:wet weight ratios before (initial) and after (final) desiccation, as well as the duration of desiccation. Because of the greater percentage of water in the inflow sediments compared to those of the outflow region, moisture loss was higher and the final dry:wet weight was lower for the former sediment type.

Table 9. Duration of desiccation, and before (initial) and after (final) dry:wet weight ratios and moisture loss, for the inflow and outflow sediments of Cell 4.

	Duration of Desiccation (hr)	Initial Dry:Wet	Final Dry:Wet	Moisture Loss
Inflow Rep A	99	0.073	0.158	2.2 x
Inflow Rep B	99	0.073	0.150	2.1 x
Outflow Rep A	72	0.160	0.234	1.5 x
Outflow Rep B	72	0.160	0.184	1.2 x

Desiccation followed by reflooding resulted in significant release of SRP from both the inflow and outflow sediments (Figure 19A,B). In terms of the total quantity of SRP released from the two sediment types, the inflow sediment, with its higher sediment P pools, released almost three times more SRP than the outflow sediment. When compared to the control sediment that was not desiccated, the amount of SRP initially released in both the Cell 4 inflow and outflow sediments was the same. The release of SRP from the control inflow sediment under the

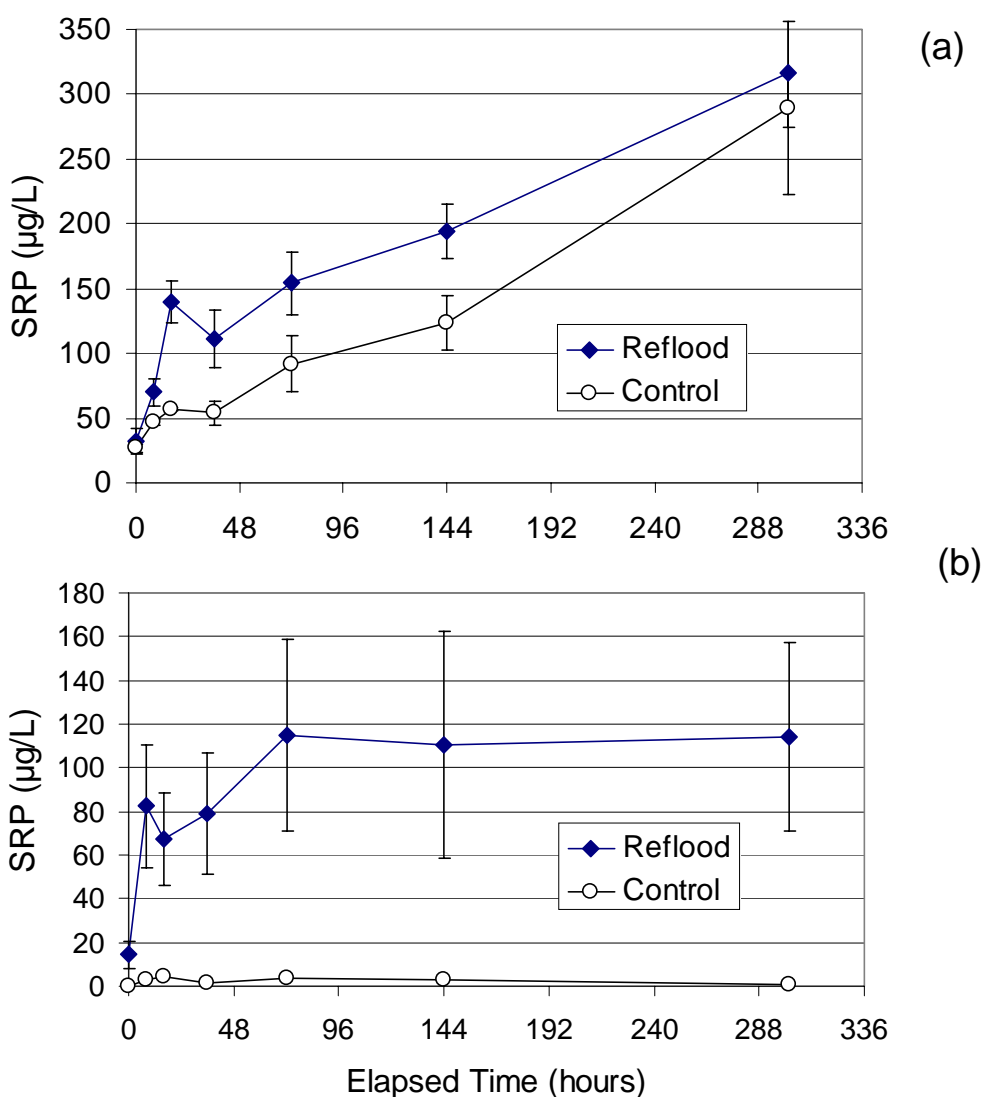


Figure 19. The release of soluble reactive P (SRP) from the desiccation of Cell 4 inflow (a) and outflow (b) sediments over 99 and 72 hours, respectively, upon reflooding with Cell 4 outflow water. The control represents a “no desiccation” treatment. Each data point represents the mean \pm s.d. of triplicate incubation vessels.

imposed oxic conditions was probably attributable to desorption and organic matter decomposition; both P pools supporting these processes are likely to be considerably higher in the inflow than outflow sediments.

These results are similar to those of Twinch (1987), who reported a decrease in the phosphate-buffering capacity and an increase in the phosphate equilibrium concentration when sediments were air-dried. This suggests that the mechanism of the SRP release for both sediment types may be desorption, although the oxidation of organic matter may have also contributed P (Qiu and McComb 1994).

High Ca and Alkalinity Concentrations

Since the outflow water from Cell 4, which was used in the incubations of both inflow and outflow sediment types, had low concentrations of Ca and alkalinity, we added both components to the outflow water to evaluate the effects of increased calcium/alkalinity levels on P release (Table 10). Three triplicate flasks of each sediment type were incubated under oxic conditions.

Table 10. Dissolved calcium and alkalinity concentrations and specific conductance values in Cell 4 inflow and outflow waters before and after Ca/alkalinity amendments.

Sediment Type	Diss. Calcium (mg/L)	Alkalinity (mg CaCO₃/L)	Sp. Cond. (µmho/cm)
Initial Inflow	38	140	893
Amended Inflow	76	260	1069
Initial Outflow	44	168	758
Amended Outflow	75	248	1296

The higher Ca and alkalinity concentrations (76 – 85 mg Ca/L and 244 – 259 mg CaCO₃/L) in the overlying water during the incubations of the inflow sediment inhibited the release of SRP relative to the control (36 – 52 mg Ca/L and 150 – 185 mg CaCO₃/L) (Figure 20a). The pH values for the treated and control sediments were similar throughout the incubation period (mean treatment pH = 8.54 and mean control pH = 8.42). This indicates that higher hardness

water *per se* (i.e. independent of pH) can reduce the release rate of SRP from sediments that have a significant pool of labile P. The formation of calcium phosphate compounds, $\text{CaCO}_3\text{-P}$ coprecipitation, or P sorption onto freshly precipitated CaCO_3 surfaces are the likely P retention mechanisms. Release of SRP from the control sediment was probably due to desorption and decomposition of organic matter under the oxic conditions.

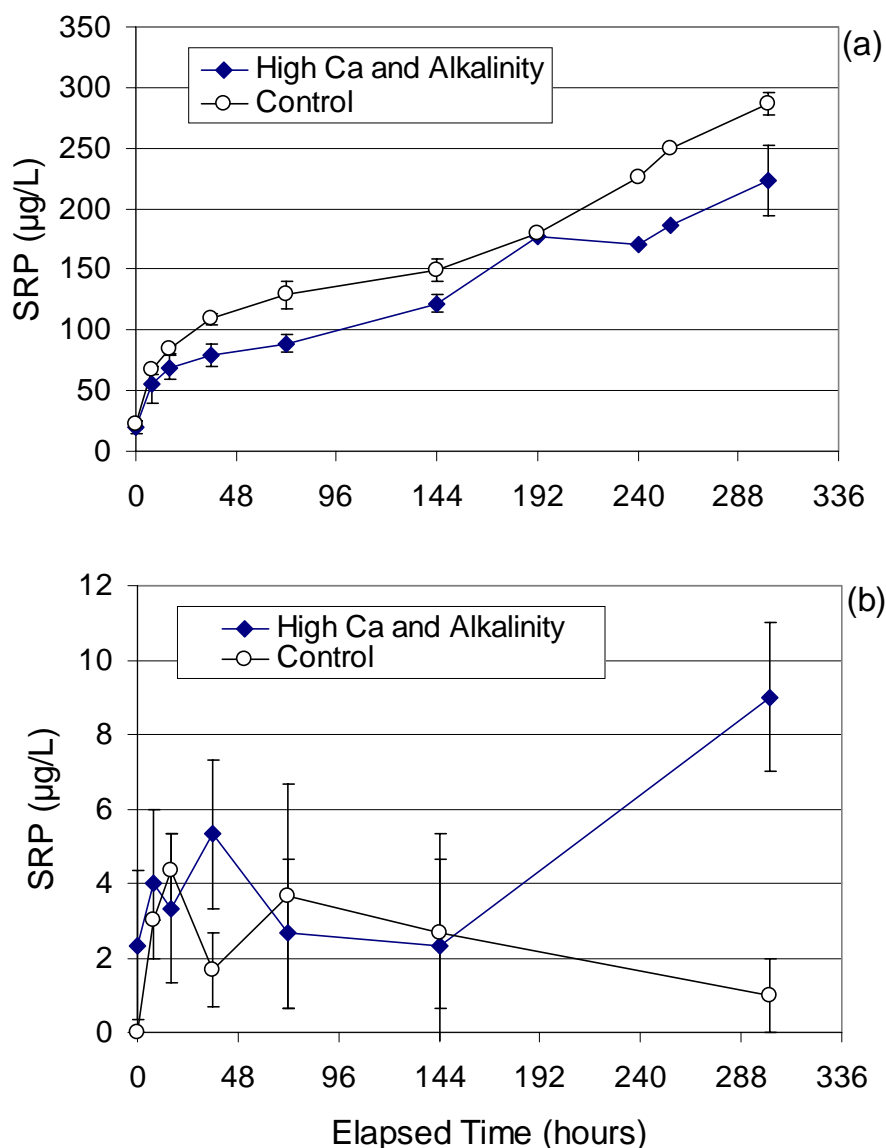


Figure 20. The release of soluble reactive P (SRP) from Cell 4 inflow (a) and outflow (b) sediments with Ca- and alkalinity-amended (75 – 76 mg Ca/L and 248 – 260 mg CaCO_3 /L) Cell 4 outflow water. The control treatment received no calcium or alkalinity amendments. Each data point represents the mean \pm s.d. from triplicate incubation vessels.

By contrast, we observed only minor differences between the release rates from outflow sediments containing high Ca and alkalinity concentrations in the overlying water and those same sediments exposed to more moderate levels of Ca and alkalinity (Figure 20b). In both the treated and control sediments, the mean SRP concentrations never exceeded 9 µg/L.

Soluble Reactive Phosphorus Amendments

The Cell 4 outflow water, which was used in the incubations for both the inflow and outflow sediments, had a SRP concentration of 2 µg/L or lower. To ascertain the potential release rate of SRP from sediments exposed to higher SRP water, we spiked the incubation waters to yield final SRP concentrations of 128 and 120 µg/L for the inflow and outflow sediment studies, respectively.

Due to the SRP spike of 128 µg/L, the initial SRP concentrations in the overlying waters of the treated and untreated (control) inflow sediments differed by 116 µg/L (Figure 21a). However, the difference in SRP concentrations between the SRP-spiked and un-spiked (control) waters narrowed throughout the incubation period; after 302 hours water column differences in SRP concentrations were indistinguishable. It therefore appears that increased SRP concentration within the overlying water temporarily hinders the release of sediment P into the water column (Figure 21a). The general increasing trend in the SRP concentrations for both the treated and control inflow sediments indicates adequate labile P pools in the sediment exist, which can be mobilized under the oxic conditions imposed in the laboratory. The nearly identical SRP concentrations for the control and SRP-spiked sediments at the end of the incubation period (Figure 21a) demonstrate the sediment has a high SRP buffering capacity.

The incubation with Cell 4 outflow sediments provided a markedly different result. In this case, the spiked SRP concentration (120 µg/L) declined asymptotically to within 12 µg/L of the un-spiked (control) sediment after 72 hours (Figure 21b). Thereafter, the SRP concentrations remained relatively constant for both the control and experimental waters. It appears that the P equilibria among the outflow sediment's exchangeable P pools and the water column favored SRP transfer from the water column into the sediment. In other words, the exchangeable sites

associated with the outflow sediment are not fully occupied by P; most of those sites are available for SRP immobilization.

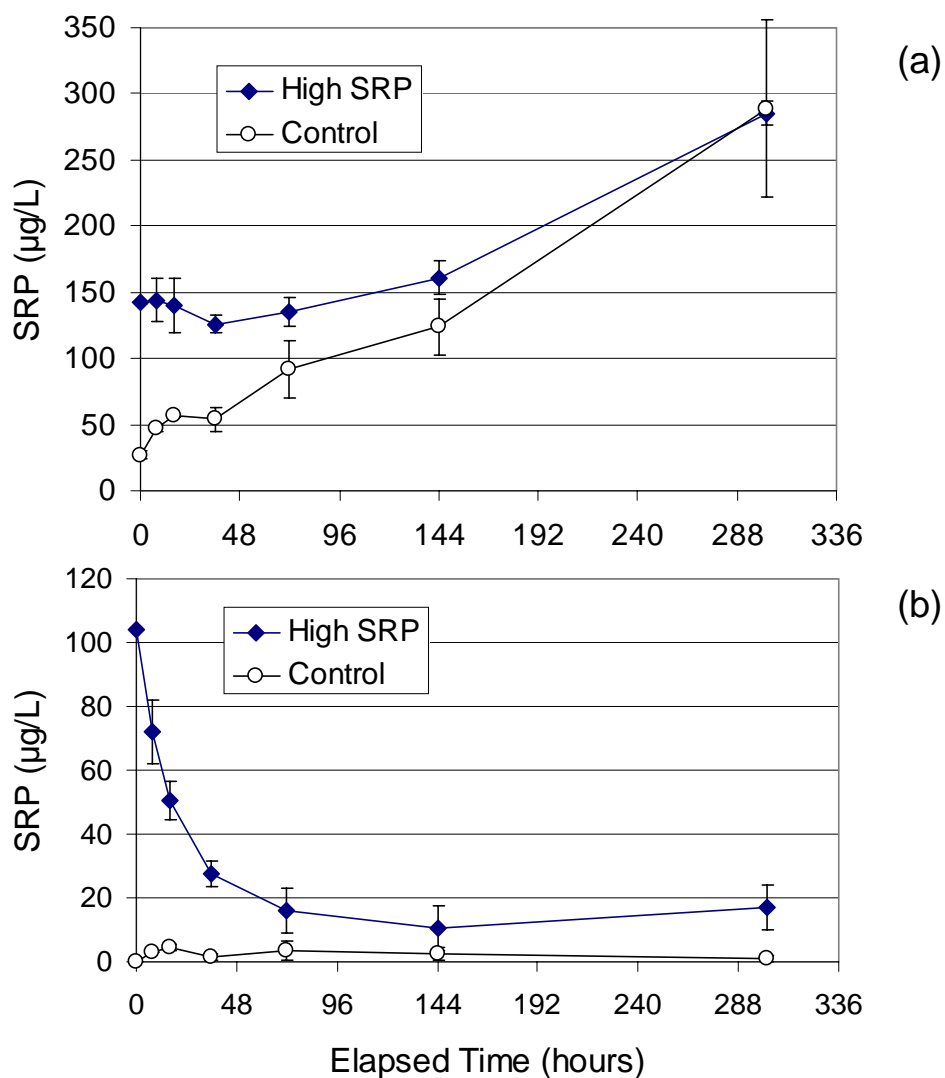


Figure 21. Soluble reactive P (SRP) concentrations for the SRP-amended and unamended overlying Cell 4 outflow water in contact with Cell 4 inflow (a) and outflow (b) sediments. The control treatment received no SRP amendments. Each data point represents the mean \pm s.d. from triplicate incubation vessels.

Sediment P Fractions and Effects of pH and Oxidic vs. Anoxic Conditions on SRP Release from Cell 4 Outflow Sediment

Compared to the inflow sediment P pools, the outflow sediments contained lower concentrations of P in each of the extracted fractions (Figure 22). This was particularly true for the labile pools (NH_4Cl -SRP, NaOH -SRP, and NaOH -org P), which undoubtedly reflects the higher loading rates of the more labile P species in the inflow region. For both sediment types, the non-labile fractions (HCl -SRP and Residue-TP) made up the majority of the sediment TP, leaving only 18 and 7 % comprising the inflow and outflow labile pools, respectively.

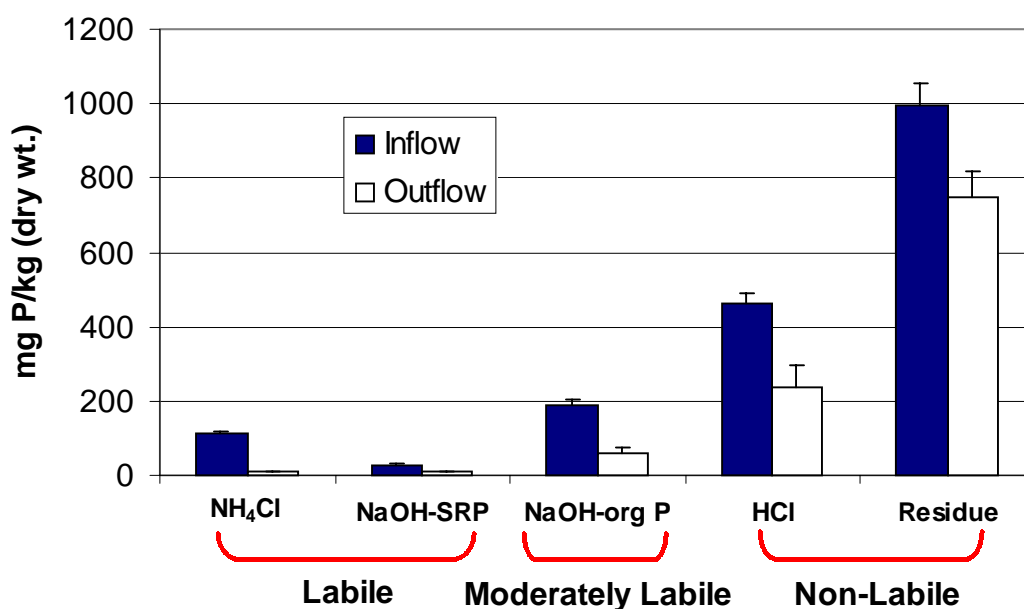


Figure 22. Inorganic P fractionation of composited Cell 4 inflow and outflow region marl sediments. Error bars indicate +1 standard deviation.

The P fractionation data help to explain the SRP release data for both sediment types. For all treatments (pH, redox, desiccation/reflooding, Ca/alk amendments, SRP spikes), the mass of SRP released from the inflow sediment was significantly higher than that released from outflow sediment. The obvious explanation is that P is removed within the Cell 4 wetland, leaving very little P to be incorporated into biomass (and ultimately, the sediments) in the outflow region.

Indeed, for each of the four pH treatments and the oxic vs. anoxic treatments, SRP releases from the outflow sediments were negligible (Figures 23 and 24), and considerably less than the releases reported for the inflow sediment under the same treatments (DBEL 2000a).

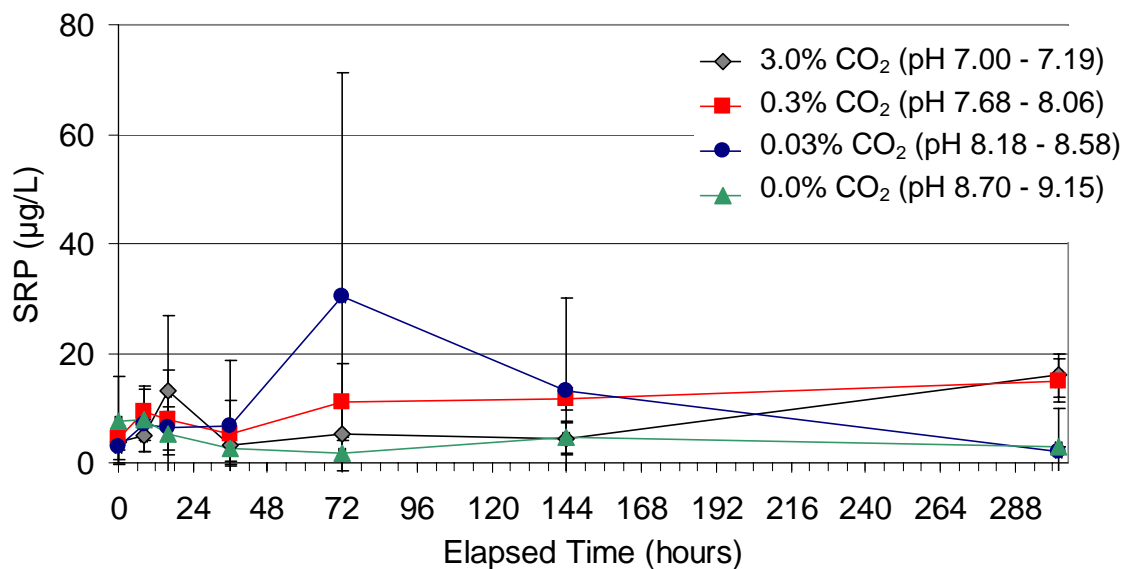


Figure 23. Time course for SRP release from Cell 4 outflow region marl sediments exposed to varying pH values. Each data point represents the mean \pm 1 s.d. of three replicates.

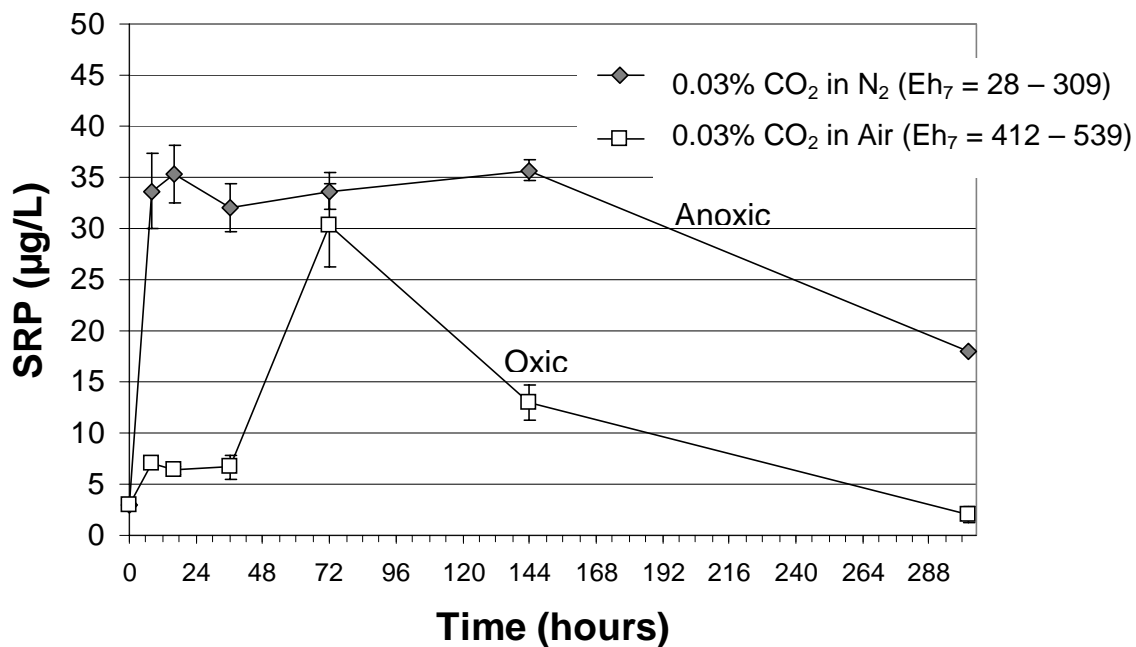


Figure 24. Time course for SRP release from Cell 4 outflow region marl sediments exposed to oxic and anoxic conditions. Each data point represents the mean \pm 1 s.d. of three replicates.

Technical Evaluation of DMSTA for Simulating TP Removal in SAV Wetlands

Background

During this reporting period, we performed a technical evaluation of the dynamic simulation model for STA design developed by Drs. Robert Kadlec and William Walker (DOI consultants). Their model has been termed the “Dynamic Model for Stormwater Treatment Areas” or DMSTA. The purpose of our effort was to provide feedback on how effectively DMSTA simulates SAV system performance. We provided this evaluation at an intermediate draft stage of DMSTA development, rather than to the final version, so that our feedback would benefit model development. Our technical evaluation of this modeling effort was performed in partial fulfillment of Task 9 in our Project Work Plan.

In June 2000, Dr. Walker provided us with a draft version of the DMSTA program. Several months earlier, we had independently programmed a model based on DMSTA for a forecasting analysis evaluating the impact of Cell 4 hydraulic enhancements on TP removal (DBEL 2000).

At the time of our analysis, the structure of DMSTA had been conceptualized but a draft version was not available (Walker 1999). We spent approximately 2 weeks coding and debugging a working version of the model and then spent several more weeks performing simulations with the model. This previous experience with DMSTA gave us a thorough understanding of the model's capabilities, strengths, and weaknesses.

We began our technical evaluation of DMSTA by comparing simulations from our version and Dr. Walker's "official" version of the program. For the comparisons we used the same input time series and model parameters. The results of the comparisons verified that DBEL's version produced identical results ($r^2 = 0.99$) as Dr. Walker's. This comparison provided a basis for using our version, which is substantially simpler (due primarily to excluding the extensive diagnostics employed by Dr. Walker), in performing this evaluation and investigating possible improvements to the model. To provide feedback on DMSTA application to SAV systems, we used the historic record from STA-1W Cell 4 for the period of January 1995 through June 2000 to construct an input file and for calibration data. We also investigated a relatively simple modification to the model structure that improved calibration compared Dr. Walker's version of DMSTA.

DMSTA Overview

The Dynamic Model for Stormwater Treatment Areas (DMSTA) is being developed specifically for design and analysis of the District's STAs and therefore must be sufficiently general to model a wide range of wetland types (e.g. emergent macrophytes, SAV, and periphyton).

We refer to DMSTA as a 'quasi-process' model because of its highly aggregated representation of generalized wetland processes (Figure 25). A true process model would contain more specific details on internal treatment processes than DMSTA. On the other hand, DMSTA elaborates significantly beyond simpler empirical models such as developed by Walker (1995) and Qian and Reckhow (1998).

DMSTA simulates long-term dynamic behavior of phosphorus removal using daily flow and TP concentration input series. The model maintains a daily water balance and can simulate non-ideal hydraulics using a tanks-in-series (TIS) approach. The model maintains a daily

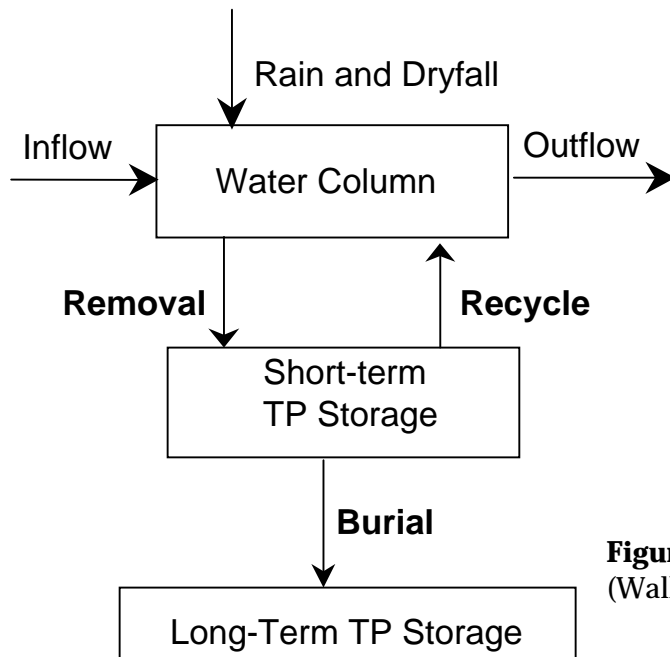


Figure 25. General model structure for DMSTA (Walker and Kadlec 2000a).

phosphorus mass balance with fluxes (removal, recycle, and burial in Figure 25) between three aggregated storage compartments: water column TP storage (SRP, DOP, PP), short-term labile P storage (biomass, new mineral and organic sediment), and long-term inactive P storage (buried sediment). TP enters the Cell 4 water column in concert with rain and influent flows and also via the recycle pathway from “labile P storage”. TP leaves the water column in concert with outflow flows and with first-order removal to the labile P storage compartment. A fraction of the modeled “short-term TP storage” is recycled to the water column, accounting for wetland processes such as desiccation, decomposition, dissolution and desorption. The recycle flux is, in essence, a dynamic background (C^*) flux. An additional fraction of “short-term TP storage” is buried to long-term inactive storage; this is the only pathway by which TP is permanently removed from the system. The model predicts a time history of outflow TP concentrations with a daily time step. Each TIS in the DMSTA model can be assigned its own coefficients, thus allowing the model to simulate sequential biological communities.

Evaluation Methods

We evaluated five different sets of equations used to represent the three principal ‘process’ flows in DMSTA (removal, recycle, and burial Figure 25). The five sets of equations are given in Table 11 and variable and parameter definitions are given in Table 12. The first four sets of

equations are included as options in the "official" version of the DMSTA program (Walker and Kadlec 2000b). The fifth set of equations was a DBEL modification aimed at improving model calibration and is not currently included as an option in the DMSTA program.

Table 11. Summary of five sets of equations evaluated for DMSTA fluxes

	Set	Description	Removal Flux	Recycle Flux	Burial Flux
"Official" DMSTA	1	1 st -order volumetric removal depth dependence	$K_v Z C$	$(1-g) K_s S$	$g K_s S$
	2	1 st -order areal removal velocity dependence	$K_a C (v+v_o)^r$	$(1-g) K_s S$	$g K_s S$
	3	2 nd -order autobiotic removal depth dependence	$K_{va} Z C$	$K_r S^2$	$K_b S$
	4	2 nd -order autobiotic removal velocity dependence	$K_{aa} C S (v+v_o)^r$	$K_r S^2$	$K_b S$
DBEL	5	1 st -order volumetric removal depth dependence seasonal dependence	$K_v Z C \text{ Seasonal}$	$(1-g) K_s S$	$g K_s S$

The first two options for DMSTA equations (Table 11) both incorporate first-order removal terms (i.e. phosphorus removal is directly proportional to water-column concentration at each time step). The difference between them is that the first set states that removal is also proportional to depth, while the second set states the removal is also proportional to flow velocity. The first model is a three-parameter model since there are three variables (K_v , K_s , and g) that must be user-defined (calibrated). The second model is essentially a five-parameter model as the velocity term adds two new user-defined parameters (v_o and r). The third and fourth sets of equations (Table 11) both incorporate second-order removal terms (i.e. removal is proportional to the product of concentration and short-term storage) and have been termed "autobiotic" models. In principal, the autobiotic model should improve calibration during start-up periods due to the dependence of removal processes on the presence of short-term (biotic) storage (Kadlec and Walker 2000b). As with the first two sets of equations, the difference between the third and fourth sets is that the third set models removal proportional to depth while the fourth set models removal proportional to velocity.

Table 12. Summary of variables and parameters for DMSTA

Variable	Units	Description	Source
C	ppb	Water column TP concentration	Calculated
S	mg/m ²	Short-term TP storage (biomass, new sediment)	Calculated
Z	m	Water depth	Calculated
v	cm/s	Flow velocity	Calculated
v _o	cm/s	Velocity effect offset	User-defined
r	-	Velocity effect exponent	User-defined
K _v	1/yr	1 st -order volumetric removal constant	User-defined
K _a	m/yr	1 st -order areal removal constant	User-defined
g	-	Fraction of short-term storage that is buried	User-defined
K _s	1/yr	Turnover rate of short-term storage	User-defined
K _{va}	1/yr/(mg/m ²)	Volumetric autotrophic removal constant	User-defined
K _{aa}	m/yr/(mg/m ²)	Areal autotrophic removal constant	User-defined
K _r	1/yr/(mg/m ²)	2 nd -order autotrophic recycle constant	User-defined
K _b	1/yr	Autotrophic burial constant	User-defined
Seasonal	-	Factor that decreases removal in winter months	User-defined

The fifth equation option (Table 11) was a straightforward modification by DBEL of the first equation option that simply included a seasonal effect on removal. In winter months, removal was modeled as less effective than during the rest of the year. The seasonal differential was modeled as a half-sine wave that lasted for 6 months with the peak (lowest removal) occurring in early March. By including a seasonal effect, this model's equations required a total of five user-specified parameters (K_v, K_s, g, and seasonality magnitude and phase). Therefore, DBEL's seasonal model has the same number of parameters (5) as the velocity dependent models (Sets 2 and 4 in Table 11) in the official DMSTA program.

The models were calibrated in two steps using the historic Cell 4 data set. First the dynamic water balance was calibrated so that DMSTA outflow and depth predictions best matched daily measured data from January 1995 through June 2000. Since all five models in our evaluation utilized the identical input time-series, the water balance was calibrated only once. The second step was to calibrate the 3 or 5 TP parameters for each of the five sets of DMSTA equations in Table 11. The parameters for each set of equations were calibrated to two separate time periods from the Cell 4 data set. The first period was using data from January 1995 through June 2000, which was the entire period of record available at the time of this study and includes the

wetland's start-up years. The second period, which uses data from June 1997 through June 2000, is more representative of steady long-term performance as it excludes the start-up years.

For the January 1995 through June 2000 calibration, values of model parameters were calibrated to minimize the following error function:

$$\text{sum of residuals} = \sum_{1995}^{\text{present}} \left| [TP]_{\text{composite data}} - [TP]_{\text{simulated composite}} \right|$$

Residuals were calculated on a weekly basis using the District's weekly composite TP data and a weekly average of daily-simulated TP concentrations. This feature (using weekly TP values for calibration) was unique to DBEL's version of DMSTA and was not included in the official DMSTA program. The calibration procedure was similar for the June 1997 through June 2000 period.

After parameters were estimated to minimize the error function, a sum-of-squares linear regression analysis (using an Excel spreadsheet) was performed between measured and simulated weekly TP values to arrive at measures for goodness-of-fit. Linear regression between simulated and measured data for a "perfect" model would have a slope equal to 1, y-intercept equal to 0, and a correlation coefficient (r^2) equal to 1.0. Here, we use the regressed slope and correlation coefficient as a goodness-of-fit measure for the model.

The DOI consultants have advocated calibrating DMSTA to TP outflow load (kg/day) as opposed to outflow concentration data (mg/L). Using their approach, outflow load is not a directly measured parameter, but is calculated as the product of outflow concentration and flow rate measurements. In DMSTA, flow rate is a calibrated model output with very good correlation to data (discussed below in water budget calibration results), whereas DMSTA simulations of outflow concentration had a much lower correlation to data (discussed below in TP calibration results). Therefore, calibration to outflow load would be biased by the higher accuracy of the flow rate calibration. Rather than rely on loadings, DBEL calibrated DMSTA using only first-hand data (flow rate and concentration) as we feel this is the most unbiased approach for goodness-of-fit measures.

DMSTA water budget calibration

Figures 26 and 27 show comparisons of DMSTA simulated G-256 outflow rates and Cell 4 water depths compared to measured data. The simulated outflow rate is a good fit to the data (Figure 26). However, water depth simulations tended to be more dynamic (variably higher and lower) than the measured data (Figure 27), particularly prior to June 1997, which is also reflected with a lower ($r^2 = 0.36$) correlation coefficient.

Calibration of DMSTA to Cell 4 TP data

Figure 28 shows a comparison of measured and simulated Cell 4 outflow TP concentrations using the equations of Set 1 (in Table 11) for January 1995 through June 2000. Figure 29 shows the same comparison for the alternate calibration period of June 1997 through June 2000. Table 13 shows a summary of calibrated parameter coefficients and goodness-of-fit measures (slope and r^2) for this and the other four cases studied for January 1995 through June 2000. Table 14 shows the same information for the alternate calibration period of June 1997 through June 2000.

During periods of relatively steady conditions, such as June 1997 through September 1999, DMSTA simulations did a good job of tracking measured data. However during periods of dynamic pulsed conditions, such as January 1995 through June 1997 and September 1999 through June 2000, DMSTA substantially under-predicted Cell 4 outflow TP concentrations (Figures 28 and 29). Although we only show the time history from this one option for DMSTA equations, this trend typified the time histories of all four options included in the official DMSTA program and studied here (first four options in Table 11). In general, DMSTA appears to predict a substantially dampened (flattened) response compared to measured data.

The goodness-of-fit measures for these four cases (first four rows in Tables 13 and 14) also reflect this tendency toward a dampened response to pulsed events. Correlation coefficients for the January 1995 through June 2000 period ranged between 0.23 - 0.27 and for the June 1997 through June 2000 period were between 0.36 - 0.41. When the slope of the predicted-versus-measured regression line is less than one, it is indicative of a model that under-predicts the dynamic range of the measured data. For the first four cases in Tables 13 and 14, the slope of the regression fit ranged between 0.20 - 0.31.

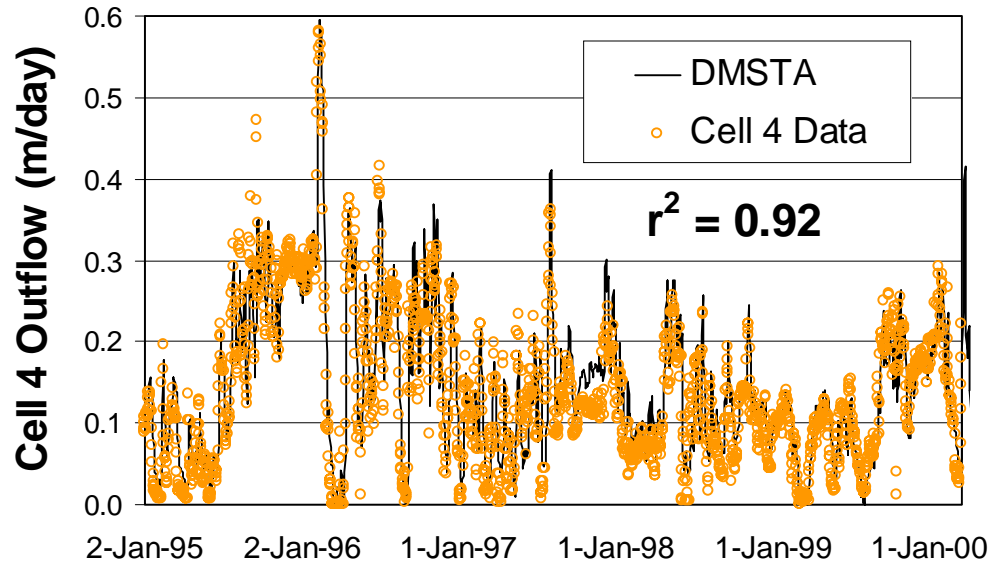


Figure 26. Comparison of simulated G-256 outflow to daily measured data.

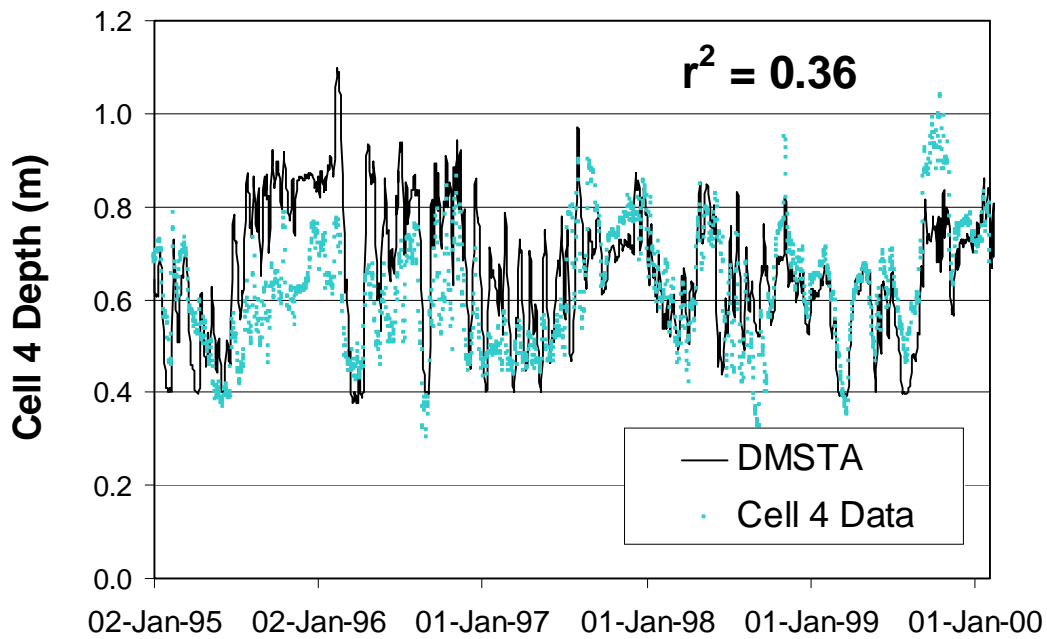


Figure 27. Comparison of simulated Cell 4 water depth to daily measured data.

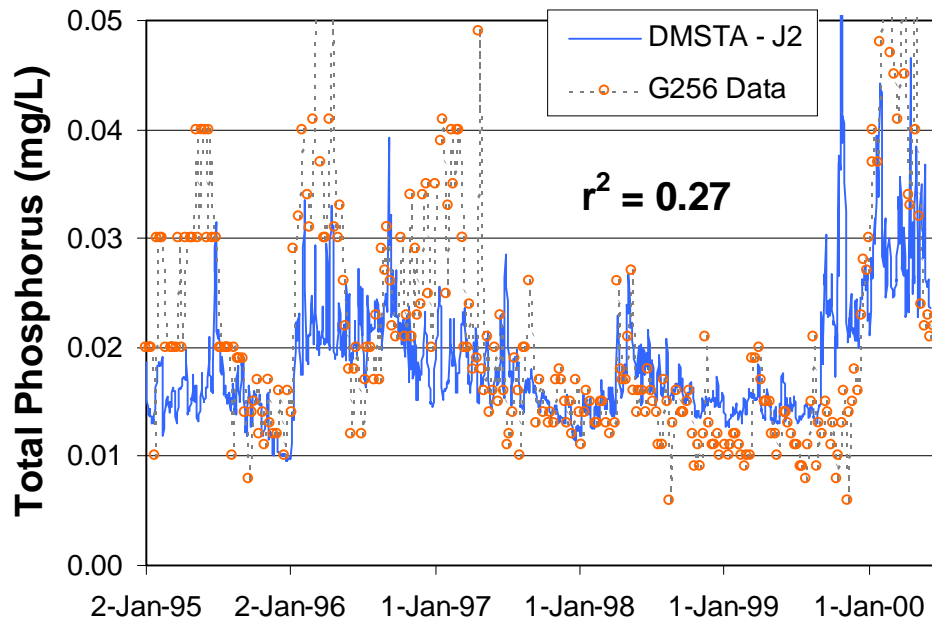


Figure 28. DMSTA TP simulation using the first-order volumetric removal option for period of January 1995 through June 2000.

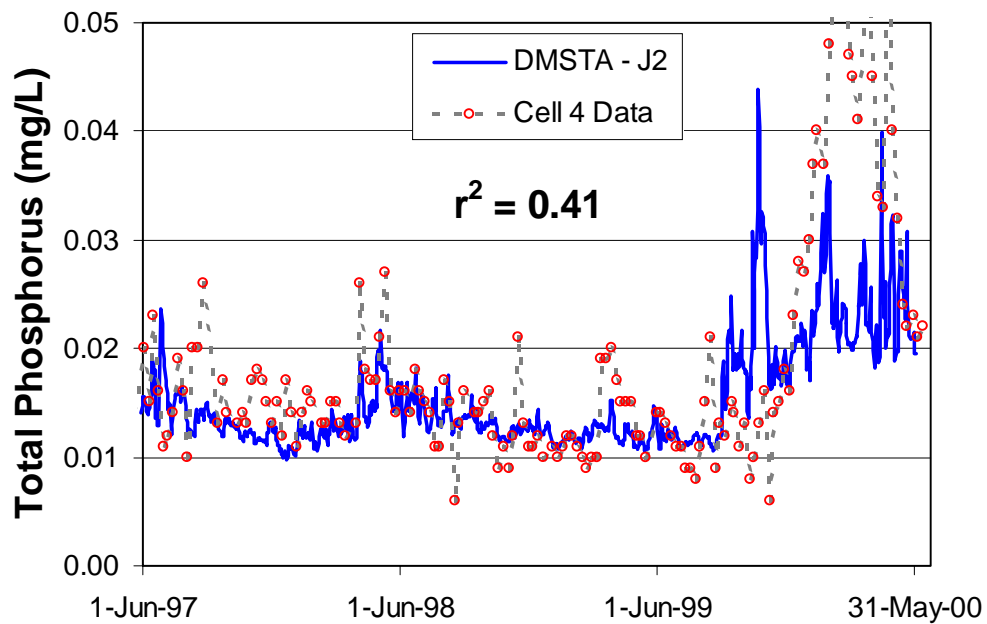


Figure 29. DMSTA TP simulation using the first-order volumetric removal option for period of June 1997 through June 2000.

Table 13. Summary of model calibrations for five options for DMSTA equations for period of 1/95 – 6/00. All calibrated parameters were established using 2 tanks-in-series (N=2) to represent Cell 4 hydraulic performance.

Option		Model Parameters										Calibration			
		1 st -order Removal Model						Autobiotic Model				Mean (ppb)	Residual (ppb)	Regression	
		K _v	K _{va}	g	K _s	Seas.	Vel.	K _v	K _{va}	K _r	K _b			r ²	Slope
"Official" DMSTA	1	220	-	0.4	2	-	-	-	-	-	-	19	7	0.27	0.26
	2	-	240	0.4	2	-	Yes	-	-	-	-	19	7	0.26	0.27
	3	-	-	-	-	-	-	.22	-	.002	1	19	7	0.23	0.19
	4	-	-	-	-	-	Yes	-	.28	.002	1	19	7	0.25	0.20
DBEL	5	240	-	0.4	2	Yes	-	-	-	-	-	20	6	0.46	0.41

Table 14. Summary of model calibrations for five options for DMSTA for period of 6/97 – 6/00

Option		Coefficients										Calibration			
		1 st -order Removal Model						Autobiotic Model				Mean (ppb)	Residual (ppb)	Regression	
		K _v	K _{va}	g	K _s	Seas.	Vel.	K _v	K _{va}	K _r	K _b			r ²	Slope
"Official" DMSTA	1	260	-	0.4	2	-	-	-	-	-	-	16	5	0.41	0.31
	2	-	260	0.4	2	-	Yes	-	-	-	-	17	5	0.40	0.33
	3	-	-	-	-	-	-	.26	-	.002	1	17	6	0.36	0.21
	4	-	-	-	-	-	Yes	-	.32	.002	1	16	6	0.36	0.20
DBEL	5	280	-	0.4	2	Yes	-	-	-	-	-	16	5	0.56	0.39

A comparison of the two calibration periods (Tables 13 and 14) indicates that DMSTA provided better simulation by excluding the wetland start-up period. For both calibration periods, the first-order removal models provided better calibration (higher r^2) than the autotrophic model; and for both first-order and autotrophic models, there was no significant benefit from employing a five-parameter model (with velocity effect) compared to the three-parameter model (with depth effect).

On the other hand, DBEL's five-parameter option for DMSTA was the only case that we studied that substantially improved model calibration (Tables 13 and 14). DBEL's seasonal model increased correlation coefficients between 50-100% compared to the four cases from the official DMSTA program. Similarly, the slope of the regression fit for the seasonal model was higher than the slope of the four official versions. Figure 30 demonstrates that the time history simulation of the outflow TP concentration is also visibly superior for the seasonal model compared to the first-order volumetric model shown in Figure 28. Also, note that the values of the mean residuals were quite similar for all five cases studied (Tables 13 and 14). This indicates that a measure such as correlation coefficient significantly enhances the ability to discern goodness-of-fit compared to evaluating residuals alone.

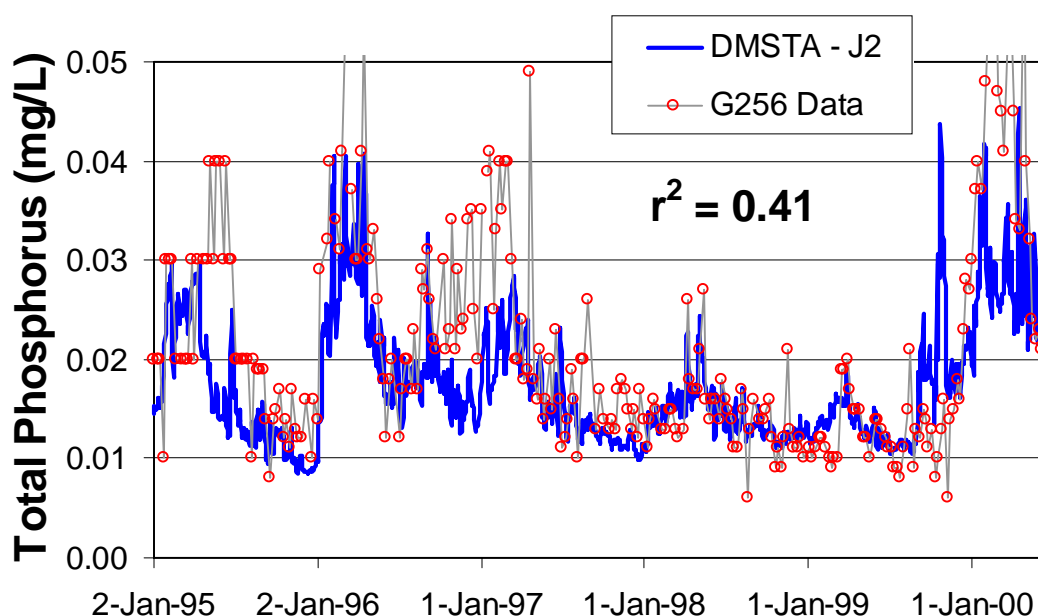


Figure 30. Seasonal effect on TP removal.

Conclusions and Recommendations

A summary of significant findings for DMSTA simulation of Cell 4 and other SAV system performance follows:

1. The predictive accuracy of all four of the model options available in the DMSTA program was marginal. For simulations that did not include wetland startup, correlation coefficients (r^2) for regressions of predicted and measured data improved ~50% to 0.36-0.41. The principal reason for these somewhat less than desirable results was the model's tendency to flatten the predicted response to pulse loading events, independent of which of the four equation options was used.
2. For both calibration periods, the first-order removal model provided slightly better simulations (higher r^2) than the autobiotic model.
3. There was no apparent advantage to incorporating a velocity effect into the model's equations.
4. If there is an advantage in minimizing the number of calibration parameters, then the three-parameter first-order volumetric removal model demonstrated the best performance for modeling Cell 4 data.
5. If it is not essential to minimize the number of calibration parameters, then DBEL has suggested an enhancement to DMSTA modeling equations, namely include a seasonal effect on TP removal, which can increase the goodness-of-fit measure (r^2) by 50-100% compared to the other cases studied. The seasonal model is a five-parameter model, which is the same number of parameters as the two equation options that included velocity effects, and is not currently supported in the DMSTA program.
6. For comparing simulation goodness-of-fit, simulation residuals are ineffective at discriminating between model options when used alone. However, when complemented with a second measure, such as correlation coefficients (r^2), effective comparisons of goodness-of-fit can be made.

Based on these findings, we make the following recommendations for DMSTA as it applies to simulating SAV systems:

1. For simulations of TP concentrations for pulse-loaded events such as is expected for STA design, the DMSTA and the modifications to it proposed by DBEL should be used with caution, as they have demonstrated only marginal predictability during dynamic events.
2. The equation options in DMSTA require further optimization. As demonstrated by DBEL's seasonal model, there exists at least one alternate and relatively simple option for DMSTA equations that leads to substantially improved model calibration. Other options for DMSTA equations must continue to be investigated and included in the DMSTA program to maximize the model's predictability and utility.
3. In addition to calculating simulation residuals during calibration, the DMSTA program should incorporate a complementary diagnostic measure such as correlation coefficients to assess goodness-of-fit of the simulation results.

References

DB Environmental (DBEL). 2000. A Demonstration of Submerged Aquatic Vegetation/Limerock Treatment System Technology for Removing Phosphorus from Everglades Agricultural Area Waters: Follow-on Study. Cell 4 Feasibility Study submitted to South Florida Water Management District and the Florida Department of Environmental Protection. West Palm Beach, FL.

Qian, S.S. and K.H. Reckhow. 1998. Modeling phosphorus trapping in wetlands using nonparametric Bayesian regression. *Water Resources Research* 34(7): 1745-1754.

Qiu, S. and A.J. McComb. 1994. Effects of oxygen concentration on phosphorus release from reflooded air-dried wetland sediments. *Aust. J. Mar. Freshwater Res.* 45: 1319 – 1328.

Twinch, A.J. 1987. Phosphate exchange characteristics of wet and dried sediment samples from a hypertrophic reservoir: implications for the measurements of sediment phosphorus status. *Water Res.* 21:1225-1230.

Walker, W.W. 1995. Design basis for Everglades stormwater treatment areas. *Water Resources Bulletin* 31(4): 671-685.

Walker, W.W. 1999. Contributions to workshop on STA/Polishing Cell Design on March 18, 1999. South Florida Water Management District, West Palm Beach, FL.

Walker, W.W. and R.H. Kadlec. 2000a. Contributions to the Everglades Technical Workshop on May 17, 2000. Sponsored by Florida Department of Environmental Protection and South Florida Water Management District, West Palm Beach, FL.

Walker, W.W. and R.H. Kadlec. 2000b. Contributions to workshop on Biological Systems for STAs on September 8, 2000. Sponsored by Florida Department of Environmental Protection and South Florida Water Management District, West Palm Beach, FL.

Task 10. Cell 5 Inoculation and Monitoring

Since October 1999, we have sampled STA-1W Cell 5 for water column P concentrations from near the influent structure (G-302). Beginning June 1, 2000, we moved our sampling station to three outfall locations of Cell 5 near the west levee to monitor outflow concentrations of TP and apparent color. The data initially showed a highly colored (\bar{x} =310 CPU) outflow with TP concentrations (\bar{x} = 171 $\mu\text{g/L}$) similar to those found near the influent between October 1999 and May 2000 (\bar{x} = 173 $\mu\text{g/L}$) (Figure 31). Beginning in July, however, TP concentrations have declined, and in October averaged 54 $\mu\text{g/L}$.

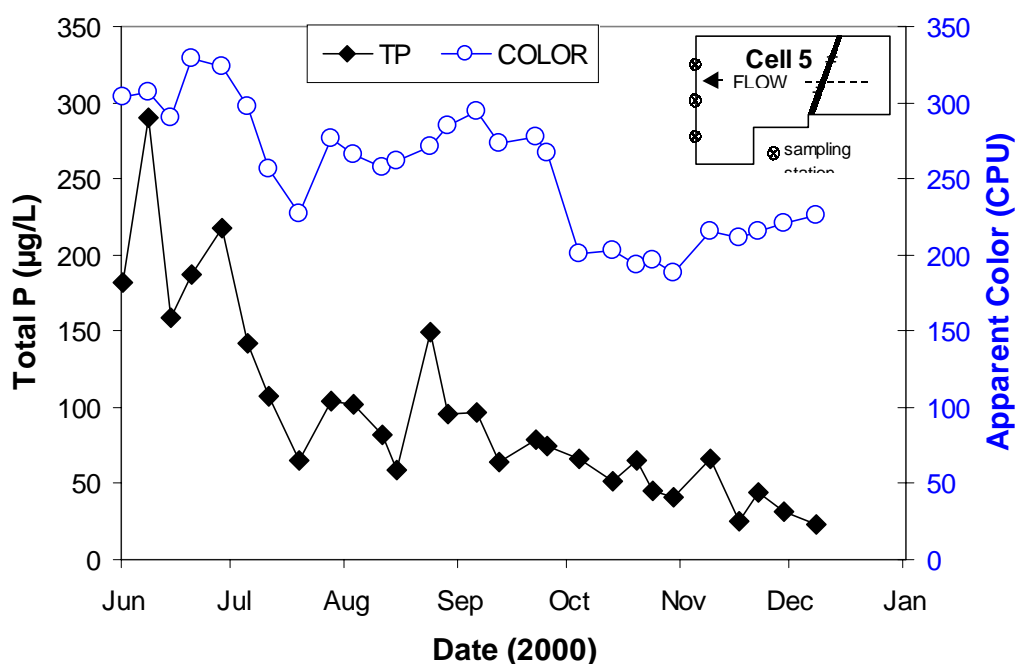


Figure 31. Total phosphorus and apparent color concentrations of surface water near the outflow of Cell 5. Each data period represents the mean of weekly grabs samples from three stations.

Our August 2000 vegetation survey of Cell 5 has revealed that SAV beds, primarily *Najas* and *Ceratophyllum*, have expanded dramatically within the wetland (Figures 32 and 33). We also recorded more *Hydrilla* in August than the previous months (Figure 34). SAV is more sparse in the northwest reaches of the cell, likely due to the high wave energy created by an unbroken

east-west fetch of several km. The low density of SAV in the southwest portion of the cell is due to the presence of large floating mats of alligator weed (*Alternanthera*).

Combining the data for declining levels of TP with an increase in SAV biomass, it appears that the SAV has reached sufficient density to ensure modest TP removal through the cell. We believe that the increase in SAV biomass in Cell 5 can lead to an increase in SRP removal by plant uptake and P coprecipitation, as well as to a decrease in particulate P export due to the dampening of wind-induced sediment resuspension.

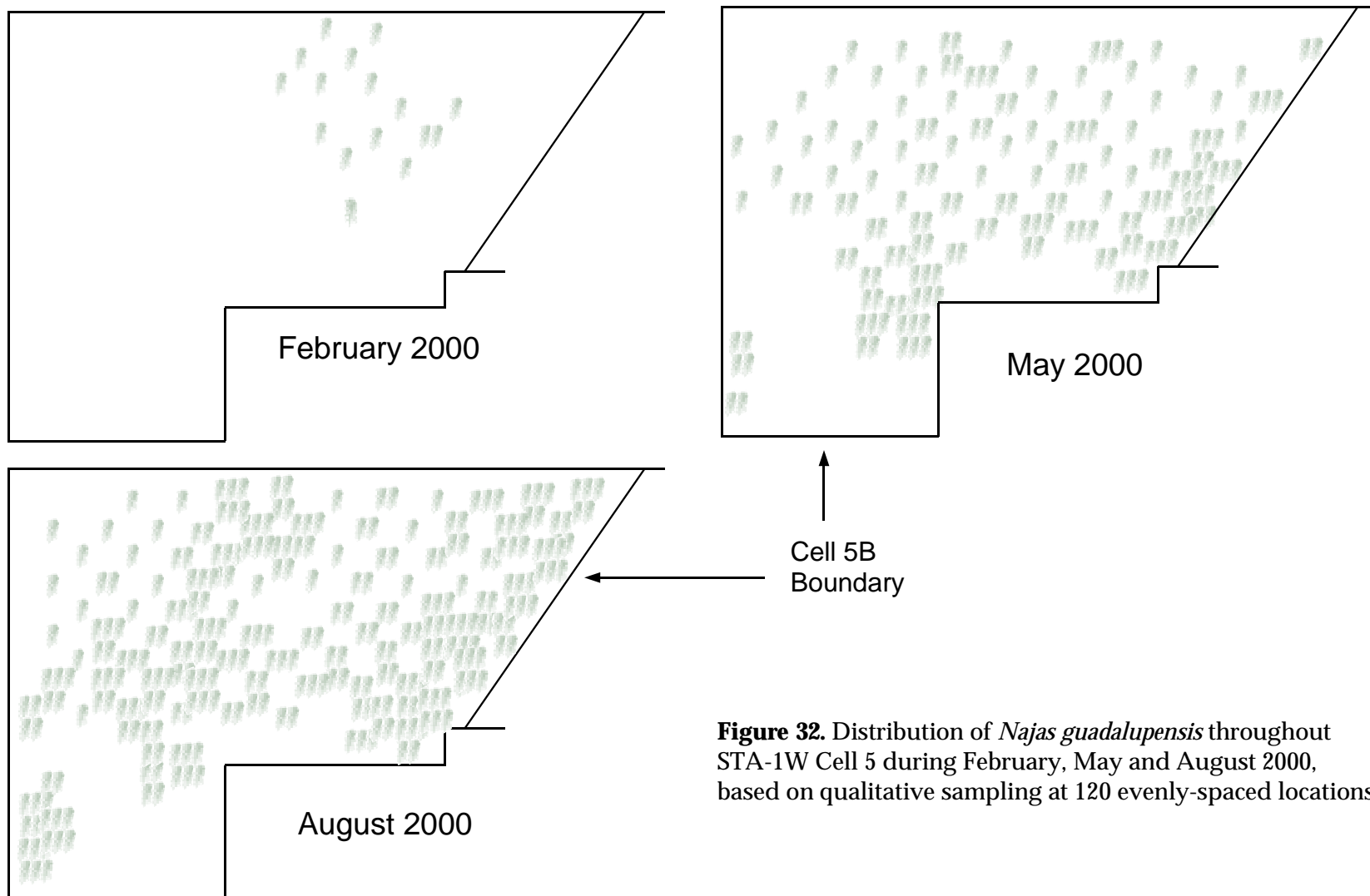


Figure 32. Distribution of *Najas guadalupensis* throughout STA-1W Cell 5 during February, May and August 2000, based on qualitative sampling at 120 evenly-spaced locations.

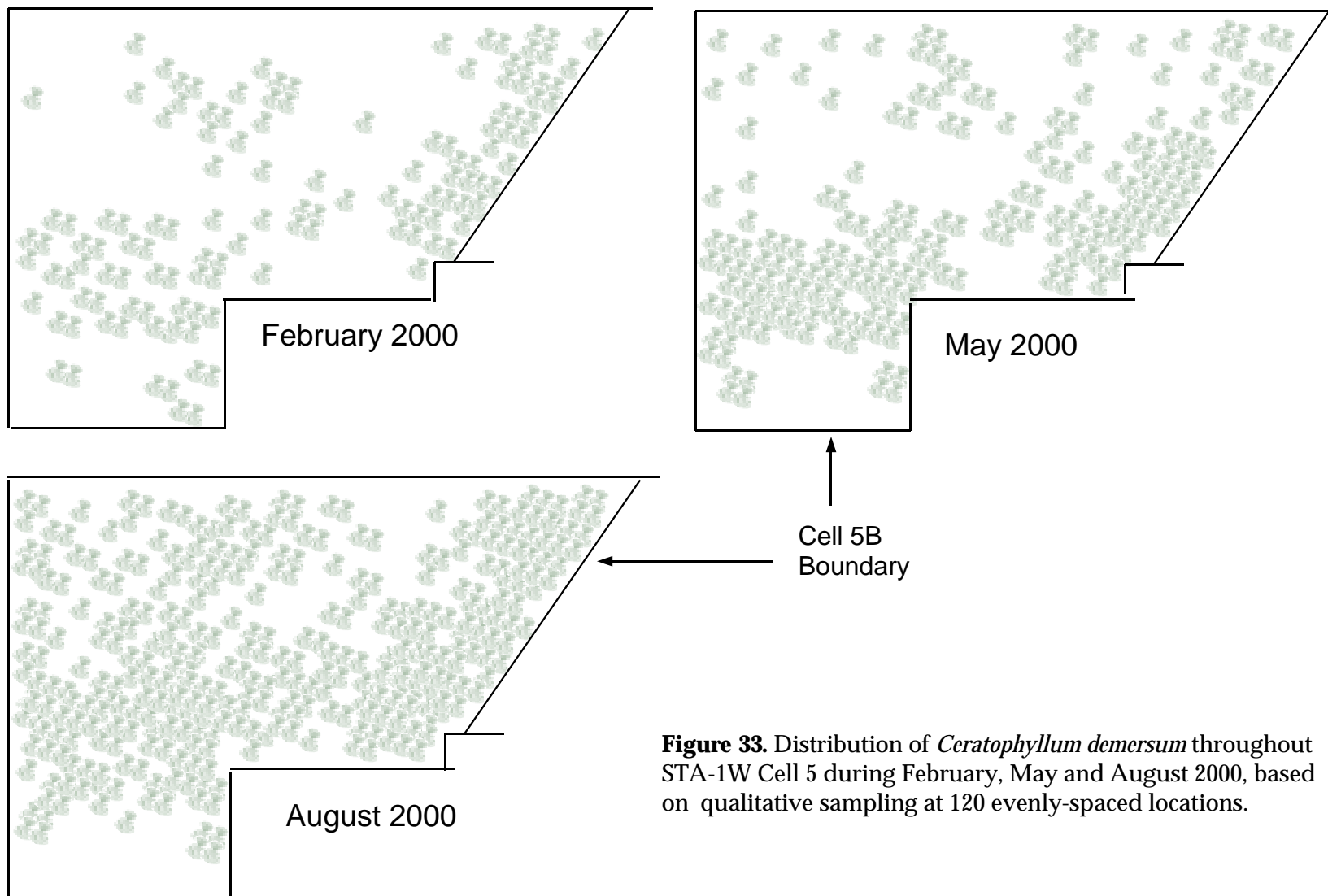


Figure 33. Distribution of *Ceratophyllum demersum* throughout STA-1W Cell 5 during February, May and August 2000, based on qualitative sampling at 120 evenly-spaced locations.

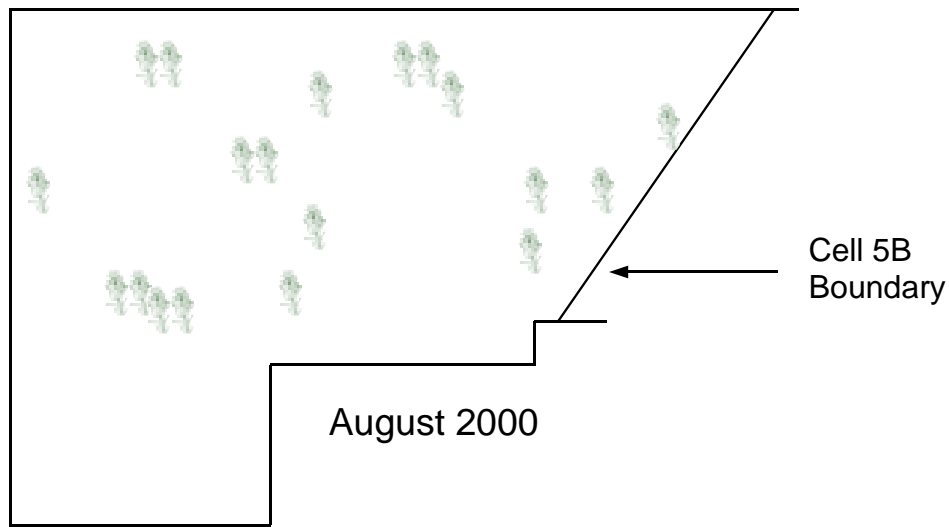


Figure 34. Distribution of *Hydrilla* throughout STA-1W Cell 5 during August 2000, based on qualitative sampling at 120 evenly-spaced locations. *Hydrilla* biomass was too sparse during February and May 2000 to be included in a distribution map for those months.